研究成果の刊行に関する一覧表

著者名	論文タイトル名	発表誌名	巻名	ページ	出版年
Midorikawa Y, Tsutsumi S, Nishimura K, Kamimura N, Kano M, Sakamoto H, Makuuchi M, Aburatani H.	Distinct chromosomal bias of gene expression signatures in the progression of hepatocellular carcinoma.	Cancer Res.	64(20)	7263-70	2004
Hippo Y, Watanabe K, Watanabe A, Midorikawa Y, Yamamoto S, Ihara S, Tokita S, Iwanari H, Ito Y, Nakano K, Nezu J, Tsunoda H, Yoshino T, Ohizumi I, Tsuchiya M, Ohnishi S, Makuuchi M, Hamakubo T, Kodama T, Aburatani H.	Identification of Soluble Amino Terminal Fragment of Glypican-3 as a Serological Marker for Early Stage Hepatocellular Carcinoma.	Cancer Res.	64(7)	2418-2423	2004
Komura D, Nakamura H, Tsutsumi S, Aburatani H, Ihara S.	Multidimensional support vector machines for visualization of gene expression data.	Bioinformatics.	21(4)	439-44	2004
Fujiwara K, Ochiai M, Ohta T, Ohki M, Aburatani H, Nagao M, Sugimura T, Nakagama H.	Global gene expression analysis of rat colon cancers induced by a food-borne carcinogen, 2-amino-1-methyl-6-phenylimidazo[4,5-b]pyridine.	Carcinogenesis.	25(8)	1495-505	2004
Sakurai S, Hasegawa T, Sakuma Y, Takazawa Y, Motegi A, Nakajima T, Saito K, Fukayama M, Shimoda T.	Myxoid epithelioid gastrointestinal stromal tumor (GIST) with mast cell infiltrations: a subtype of GIST with mutations of platelet-derived growth factor receptor alpha gene.	Hum Pathol,	35	1223-30	2004
Goto A, Niki T, Terado Y, Fukushima J, Fukayama M.	Prevalence of CD99 protein expression in pancreatic endocrine tumours (PETs).	Histopathology.	45	384-92	2004
Goto A, Niki T, Moriyama S, Funata N, Moriyama H, Nishimura Y, Tsuchida R, Kato JY, Fukayama M. Immunohistochemical study of Skp2 and Jab1, two key molecules in the degradation of P27, in lung adenocarcinoma.	Pathol Int,	Pathol. Int.	54	675-81	2004
Sakuma K, Chong JM, Sudo M, Ushiku T, Inoue Y, Shibahara J, Uozaki H, Nagai H, Fukayama M.	High-density methylation of p14ARF and p16INK4A in Epstein-Barr virus-associated gastric carcinoma.	Int J Cancer,	112	273-8	2004
Koshiishi N, Chong JM, Fukasawa T, Ikeno R, Hayashi Y, Funata N, Nagai H, Miyaki M, Matsumoto Y, Fukayama M.	p300 gene alterations in intestinal and diffuse types of gastric carcinoma.	Gastric Cancer.	7(2)	85-90	2004
Shibahara J, Todo T, Morita A, Mori H, Aoki S, Fukayama M.	Papillary neuroepithelial tumor of the pineal region. A case report.	Acta Neuropathol (Berl).	108	337-40	2004

Ishikawa S, Uozumi N, Shiibashi T, Izumi T, Fukayama M, Shimizu T, Watanabe J, Nogami S.	Short report: Lethal malaria in cytosolic phospholipase A2- and phospholipase A2IIA-deficient mice.	Am J Trop Med Hyg,	70	645-50	2004
Shibahara J, Goto A, Niki T, Tanaka M, Nakajima J, Fukayama M.	Primary pulmonary paraganglioma: report of a functioning case with immunohistochemical and ultrastructural study.	Am J Surg Pathol,	28	825-9	2004
Dobashi Y, Goto A, Fukayama M, Abe A, Ooi A.	Overexpression of cdk4/cyclin D1, a possible mediator of apoptosis and an indicator of prognosis in human primary lung carcinoma.	Int J Cancer,	110	532-41	2004
Uemura K, Nakajima M, Yamauchi N, Fukayama M, Yoshida K.	Sudden death of a patient with primary hypereosinophilia, colon tumours, and pulmonary emboli.	J Clin Pathol,	57	541-3	2004
金子順一, 菅原準彦, 新谷隆, 松井郁一, 赤松延久, 岸庸二, 竹村信行, 佐野圭二, 今村宏, 國土典宏, 幕内雅敏, 元井亨, 深山正久.	C型肝炎肝硬変に対する生体肝移植後,約1年6ヵ月で肝硬変に至り,再移植を施行した1例.	今日の移植	17	829-830	2004
Hasegawa K, Kokudo N, Makuuchi M.	Advances in surgical therapy for hepatocellular carcinoma.	Gan To Kagaku Ryoho.	31	2110-3	2004
Li X, Hui AM, Sun L, Hasegawa K, Torzilli G, Minagawa M, Takayama T, Makuuchi M.	p16INK4A hypermethylation is associated with hepatitis virus infection, age, and gender in hepatocellular carcinoma.	Clin Cancer Res.	10	7484-9	2004
Torzilli G, Gambetti A, Del Fabbro D, Leoni P, Olivari N, Donadon M, Montorsi M, Makuuchi M.	Techniques for hepatectomies without blood transfusion, focusing on interpretation of postoperative anemia.	Arch Surg.	139	1061-5	2004
Torzilli G, Del Fabbro D, Olivari N, Calliada F, Montorsi M, Makuuchi M.	Contrast-enhanced ultrasonography during liver surgery.	Br J Surg.	91	1165-7	2004
Minagawa M, Makuuchi M, Takayama T, Kokudo N.	Surgical approach to liver metastasis with hepatic hilar invasion.	Hepatogastroenterology.	51	1467-9	2004
Minagawa M, Makuuchi M, Kubota K, Kondo Y.	Intraoperative three-dimensional visualization of liver vasculature by ultrasonography.	Hepatogastroenterology.	51	1448-50	2004
Chiappa AC, Makuuchi M, Zbar AP, Biella F, Vezzoni A, Torzilli G, Andreoni B.	Protective effect of methylprednisolone and of intermittent hepatic pedicle clamping during liver vascular inflow occlusion in the rat.	Hepatogastroenterology.	51	1439-44	2004
Sondenaa K, Kubota K, Sano K, Takayama T, Makuuchi M.	Successful reconstruction of segmental or subsegmental bile ducts after resection of hilar bile ducts: short- and long-term results.	Hepatogastroenterology.	51	1278-81	2004

Yuan LW, Tang W, Kokudo N, Sugawara Y, Karako H, Hasegawa K, Aoki T, Kyoden Y, Deli G, Li YG, Makuuchi M.	Measurement of des-gamma-carboxy prothrombin levels in cancer and non-cancer tissue in patients with hepatocellular carcinoma.	Oncol Rep.	12	269-73	2004
Aoki T, Imamura H, Hasegawa K, Matsukura A, Sano K, Sugawara Y, Kokudo N, Makuuchi M.	Sequential preoperative arterial and portal venous embolizations in patients with hepatocellular carcinoma.	Arch Surg.	139	766-74	2004
Miyoshi H, Fujie H, Moriya K, Shintani Y, Tsutsumi T, Makuuchi M, Kimura S, Koike K.	Methylation status of suppressor of cytokine signaling-1 gene in hepatocellular carcinoma.	J Gastroenterol.	39	563-9	2004
Hasegawa K, Imamura H, Akahane M, Miura Y, Kiryu S, Ohtomo K, Makuuchi M.	Administration of iodized oil resulted in impaired liver function due to enhanced portosystemic shunting.	Cardiovasc Intervent Radiol.	27	282-4	2004
Kokudo N, Imamura H, Sugawara Y, Sakamoto Y, Yamamoto J, Seki M, Makuuchi M.	Surgery for multiple hepatic colorectal metastases.	J Hepatobiliary Pancreat Surg.	11	84-91	2004
Imamura H, Seyama Y, Kokudo N, Aoki T, Sano K, Minagawa M, Sugawara Y, Makuuchi M.	Single and multiple resections of multiple hepatic metastases of colorectal origin.	Surgery.	135	508-17	2004
Sakamoto Y, Yamamoto J, Kosuge T, Sugawara Y, Seki M, Kokudo N, Azekura K, Yamaguchi T, Muto T, Makuuchi M.	Extended left hepatectomy by severing all major hepatic veins with reconstruction of the right hepatic vein.	Surg Today.	34	482-4	2004
Kusaka K, Imamura H, Tomiya T, Makuuchi M.	Factors affecting liver regeneration after right portal vein embolization.	Hepatogastroenterology.	51	532-5	2004
Kokudo N, Makuuchi M.	Current role of portal vein embolization/hepatic artery chemoembolization.	Surg Clin North Am.	84	643-57	2004
Sakamoto Y, Yamamoto J, Saiura A, Koga R, Kokudo N, Kosuge T, Yamaguchi T, Muto T, Makuuchi M.	Reconstruction of hepatic or portal veins by use of newly customized great saphenous vein grafts.	Langenbecks Arch Surg.	389	110-3	2004
Aoki T, Sugawara Y, Imamura H, Seyama Y, Minagawa M, Hasegawa K, Kokudo N, Makuuchi M.	Hepatic resection with reconstruction of the inferior vena cava or hepatic venous confluence for metastatic liver tumor from colorectal cancer.	J Am Coll Surg.	198	366-72	2004
Torzilli G, Olivari N, Moroni E, Del Fabbro D, Gambetti A, Leoni P, Montorsi M, Makuuchi M.	Contrast-enhanced intraoperative ultrasonography in surgery for hepatocellular carcinoma in cirrhosis.	Liver Transpl.	10	S34-8	2004
Torzilli G, Olivari N, Del Fabbro D, Leoni P, Gendarini A, Palmisano A, Montorsi M, Makuuchi M.	Indication and contraindication for hepatic resection for liver tumors without fine-needle biopsy: validation and extension of an Eastern approach in a Western community hospital.	Liver Transpl.	10	S30-3	2004

Inoue K, Takayama T, Higaki T, Watanabe Y, Makuuchi M.	Clinical significance of early hepatocellular carcinoma.	Liver Transpl.	10	S16-9	2004
Torzilli G, Belghiti J, Makuuchi M.	Differences and similarities in the approach to hepatocellular carcinoma between Eastern and Western institutions.	Liver Transpl.	10	S1-2	2004
Sakamoto Y, Yamamoto J, Kokudo N, Seki M, Kosuge T, Yamaguchi T, Muto T, Makuuchi M.	Bloodless liver resection using the monopolar floating ball plus ligasure diathermy: preliminary results of 16 liver resections.	World J Surg.	28	166-72	2004
堤修一,井原茂男,油谷浩幸	アレイ技術とがん研究	血液,腫瘍科	48	182-189	2004
Hippo Y, Sato S, Aburatani H.	Glypican-3 as a serum marker for hepatocellular carcinoma.	Cancer Res.	65(1)	372; 372-3	2005
Kano M, Tsutsumi S, Kawahara N, Wang Y, Mukasa A, Kirino T, Aburatani H.	A meta-clustering analysis indicates distinct pattern alteration between two series of Gene Expression profiles for induced ischemic tolerance in rats.	Physiol. Genomics.	21(2)	274-83	2005
Fukumoto S, Yamauchi N, Moriguchi H, Hippo Y, Watanabe A, Shibahara J, Taniguchi H, Ishikawa S, Ito H, Yamamoto S, Iwanari H, Hironaka M, Ishikawa Y, Niki T, Sohara Y, Kodama T, Nishimura M, Fukayama M, Dosaka-Akita H, Aburatani H.	Over-expression of The Aldo-keto Reductase Family Protein AKR1B10 Is Highly Correlated with Smokers1 Non-Small Cell Lung Carcinomas.	Clin Cancer Res.	11(5)	1776-85	2005
Aburatani H.	Discovery of a new biomarker for gastroenterological cancers.	J gastroenterol	40	1-6	2005
Yamauchi N, watanabe A, Hishinuma M, Ohashi K, Midorikawa Y, Morishita Y, Niki T, Shibahara J, Mori M, Makuuchi M, Hippo Y, Kodama T, Iwanari H, Aburatani H, Fukayama M.	The Glypican 3 oncofetal protein is a promising diagnostic marker for hepatocellular carcinoma.	Modern Pathol.	in press		
Ge X,Yamamoto S, Tsutsumi S, Midorikawa Y, Ihara S, Wang SM, Aburatani H.	Interpreting expression profiles of cancers by genome-wide survey of breadth-of-expression in normal tissues.	Genomics	in press		

Int. J. Cancer: **109**, 194–199 (2004)

Publication of the International Union Against Cancer

PROMOTER HYPERMETHYLATION OF *E-CADHERIN* AND ITS ABNORMAL EXPRESSION IN EPSTEIN-BARR VIRUS-ASSOCIATED GASTRIC CARCINOMA

Makoto SUDO[1,2], Ja-Mun CHONG[1], Kazuya SAKUMA[3], Tetsuo USHIKU[1], Hiroshi UOZAKI[1], Hideo NAGAI[3], Nobuaki FUNATA[4], Yoshiro MATSUMOTO[2] and Masashi FUKAYAMA[2]*

[1]*Department of Pathology, Graduate School of Medicine, University of Tokyo, Tokyo, Japan*
[2]*First Department of Surgery, University of Yamanashi, Yamanashi, Japan*
[3]*Department of Surgery, Jichi Medical School, Tochigi, Japan*
[4]*Department of Pathology, Tokyo Metropolitan Komagome Hospital, Tokyo, Japan*

Promoter hypermethylation of various tumor-related genes is extremely frequent in Epstein-Barr virus (EBV)-associated gastric carcinoma (EBVaGC). To investigate the significance of the promoter methylation in EBVaGC, we focused on one of the important proteins in the carcinogenesis of the stomach, E-cadherin. Methylation-specific PCR analysis (MSP) was applied to surgically resected gastric carcinomas, together with immunohistochemistry, PCR-based analysis of mutations and allelic loss, and site-specific MSP of *E-cadherin* gene. By MSP, nearly all of the carcinomas showed aberrant methylation of *E-cadherin* promoter in EBVaGC (21/22), and the frequency of this aberration was significantly higher than that in EBV-negative gastric carcinoma (GC; 45/81; $p = 0.0003$). According to immunohistochemistry of E-cadherin, the frequency of abnormal staining pattern in EBVaGC (87%) was comparable to that in the diffuse type (80%), but higher than that in the intestinal type of EBV-negative GC (47%). Promoter methylation was well correlated with abnormal staining pattern in EBVaGC, but not in EBV-negative GC. Neither mutation nor allelic loss of *E-cadherin* was observed in EBVaGC. Methylation status of *E-cadherin* within each carcinoma was heterogeneous as far as examined. Thus, in addition to the known association involving p16, we determined that promoter methylation-mediated silencing of *E-cadherin* gene was also closely associated with the development of EBVaGC, although it becomes heterogeneous within a given tumor along its progression.

Key words: *Epstein-Barr virus; gastric carcinoma;* E-cadherin; *methylation*

Epstein-Barr virus (EBV)-associated gastric carcinoma (EBVaGC) is a unique type of gastric carcinoma (GC) that accounts for 5–18% of GCs reported around the world. EBV-encoded small RNA (EBER) is present in nearly all of the carcinoma cells in the intramucosal stage. EBV in EBVaGC is monoclonal by Southern blot hybridization analysis with probes adjacent to the unique terminal repeat of EBV DNA. EBVaGC also has some characteristic clinicopathologic features, such as male preference, predominant involvement of the proximal stomach, frequent accompaniment of atrophic gastritis, a moderately differentiated tubular or poorly differentiated solid type of histology[1–3] and specific expression of the splice variants of CD44 and IL-1β.[4,5] Given these many distinctions, the carcinogenic process of EBVaGC is thought to be quite different from that of EBV-negative GC.

EBV nuclear antigen 2 (EBNA2) and latent membrane protein 1 (LMP1) are latency gene products of EBV. The former is capable of immortalizing human lymphocytes, the latter capable of transforming rodent fibroblasts. Since neither is expressed in EBVaGC,[6,7] genetic or epigenetic alterations of the infected cells might be directly responsible for the development of EBVaGC. In an investigation of the genetic changes, the deletion of 5q and/or 17p and the microsatellite instability were found to be extremely rare in EBVaGC, but very frequent in EBV-negative GC.[8] On the other hand, Kang *et al.*[9] and our own group[10] recently demonstrated that promoter hypermethylation of various tumor-related genes occurs much more frequently in EBVaGC than in EBV-negative GC. The subsequent reduction of gene expression has been observed in at least one tumor suppressor gene, *p16*.[11]

In the present study, we focused on E-cadherin, another protein important in the carcinogenesis of the stomach. E-cadherin is a Ca^{2+}-dependent cell-cell adhesion molecule that plays an essential role in the formation and maintenance of the normal architecture and function of epithelial tissues.[12–14] Abnormalities of the gene and gene expression of E-cadherin have been frequently observed in gastric carcinoma,[15–20] and the germline mutation was identified in the hereditary diffuse gastric carcinoma kindred.[21] However, few studies have correlated abnormalities of E-cadherin with the EBV infection.[22] In the present study, to clarify the significance of the promoter hypermethylation of *E-cadherin* in EBVaGC, we demonstrated its clinicopathologic features and its characteristic gene expression in GC with and without EBV infection, together with the specific analyses of *E-cadherin* gene in EBVaGC, such as genetic abnormalities, and regional heterogeneity of methylation status.

MATERIAL AND METHODS

The materials consisted of 103 gastric carcinomas that had been surgically resected at Jichi Medical School or Tokyo Metropolitan Komagome Hospital from 1988 to 1998. Fresh tissues of gastric carcinoma were frozen in liquid nitrogen immediately after surgical resection and stored at −80°C until use. Histologic typing of the carcinoma and the pathology of the resected stomachs were evaluated according to the Japanese Classification of Gastric Carcinoma.[23] We also adopted Lauren's classification of gastric carcinoma,[24] intestinal and diffuse.

To determine the presence or absence of EBV, EBER *in situ* hybridization was applied to the formalin-fixed and paraffin-embedded sections as described previously.[3] Genomic DNA was isolated from the frozen tissues by a standard phenol/chloroform

Abbreviations: EBER, Epstein-Barr virus-encoded small RNA; EBV, Epstein-Barr virus; EBVaGC, Epstein-Barr virus-associated gastric carcinoma; GC, gastric carcinoma; LOH, loss of heterozygosity; MSP, methylation-specific polymerase chain reaction; PCR-SSCP, polymerase chain reaction-single-strand conformational polymorphism.

Grant sponsor: Grant-in Aid for Scientific Research on Priority Areas, Ministry of Education, Culture, Sports, Science, and Technology of Japan.

*Correspondence to: Department of Pathology, Graduate School of Medicine, University of Tokyo, 7-3-1 Hongo, Bunkyo-ku, Tokyo 113-0033, Japan. Fax: +81-3-3815-8379. E-mail: mfukayama-tky@umin.ac.jp

Received 26 May 2003; Revised 24 September 2003; Accepted 1 October 2003

DOI 10.1002/ijc.11701

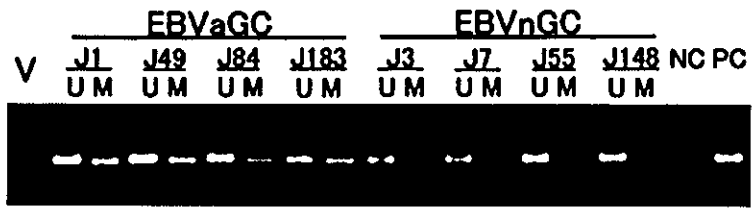

FIGURE 1 – MSP analysis of promoter hypermethylation of *E-cadherin* gene in EBV-associated and EBV-negative gastric carcinoma. Representative result of MSP of 4 EBVaGC cases (J1, J49, J84 and J183) and 4 EBV-negative GC (EBVnGC; J3, J7, J55 and J148). All 4 EBVaGC cases and 1 EBV-negative GC case (case J7) were considered methylation-positive. U, unmethylated primer set; M, methylated primer set; V, DNA marker V; NC, negative control; PC, positive control.

procedure. Due to limited sample size and relatively long duration of the tissue storage, DNA, but not RNA, could be used for the mutation analysis.

Methylation-specific polymerase chain reaction of E-cadherin gene promoter

Bisulfite modification of genomic DNA was performed[25] with the CpGenome DNA modification kit (Intergen, Purchase, NY) before the methylation-specific polymerase chain reaction (MSP) of the *E-cadherin* promoter. MSP was performed with the CpG WIZ E-cadherin Amplification kits (Intergen) according to the manufacturer's recommendation with slight modifications.[26] Reaction buffer at a final volume of 12.5 μl contained 1 unit of AmpliTaq Gold DNA polymerase (Applied Biosystems, Foster City, CA) and 1 μl of modified DNA. The temperature profiles for the amplification were as follows: initial heating at 95°C for 10 min, 40 cycles of denaturation at 95°C for 45 sec, annealing at 60°C for 45 sec and extension at 72°C for 1 min, followed by a final extension at 72°C for 10 min. A pair of positive (universal methylated and unmethylated DNA; Intergen) and negative controls (distilled water) accompanied every amplification reaction; 6 μl of each PCR product was electrophoresed in a 2% agarose gel, stained with ethidium bromide and visualized under an ultraviolet illuminator. All experiments were performed in duplicate.

Immunohistochemistry of E-cadherin

Since the high incidence of *E-cadherin* promoter hypermethylation was observed in EBVaGC, immunohistochemistry of E-cadherin was further performed to evaluate the expression of E-cadherin. For the further analysis of immunohistochemistry, the formalin-fixed and paraffin-embedded sections were available for EBVaGC when the size of the carcinoma was more than 1 cm (15 cases). For EBV-negative GCs, the specimens of Jichi Medical School were subjected to immunohistochemistry (19 intestinal and 15 diffuse type, respectively). Sections 4 μm thick were cut from formalin-fixed and paraffin-embedded specimens, deparaffinized in xylene and rehydrated in alcohol. The sections were autoclaved in 0.01 M citrate-phosphate buffer (pH 6.0) with 0.1% of Tween20 at 121°C for 10 min for antigen retrieval. The monoclonal antibody to human E-cadherin (clone HECD-1, TaKaRa, Shiga, Japan) was applied to the sections and incubated at room temperature for 1 hr. Following blockage of endogenous peroxidase activity by treatment with 0.3% hydrogen peroxide in methanol for 10 min, a standard avidin-biotin immunoperoxidase technique was used for visualization of the reactive product.[27,28] The sections were incubated with avidin-biotin complex (Vectorstain ABC kit, Vector Laboratories, Burlingame, CA), developed in 3′-3′ diaminobenzidine, counterstained with Mayer's hematoxylin for 5 min and dehydrated in alcohol prior to mounting. The epithelium of noncancerous parts within each section (if available) and/or normal colonic epithelium served as positive controls. To obtain negative controls, the primary antibodies were omitted.

For the evaluation of the immunohistochemical results, we classified the staining patterns into 3 categories according to classification recommended by Oka *et al.*[17] Tumors showing positive signal in more than 90% of tumor cells were classified as the normal type, those showing positive signal in 10–90% of tumor cells were classified as the heterogeneous type and those expressing very weak or no signal (less than 10%) were classified as the reduced type. Both reduced and heterogeneous types were considered abnormal.

TABLE I – CORRELATION BETWEEN PROMOTER HYPERMETHYLATION OF *E-CADHERIN* AND CLINICOPATHOLOGIC FACTORS IN GASTRIC CARCINOMA

Clinicopathologic factors	Promoter methylation status		*p*
	Methylated	Unmethylated	
EBV infection			
EBVaGC	21	1	0.0003
EBVnGC[a]	45	36	
Mean age	61.6 ± 14.0	64.9 ± 11.5	NS
Gender (male:female)	48:18	32:5	NS
Histology			
Intestinal	26	22	0.0502
Diffuse	40	15	
Location[b]			
Upper and middle	51	24	NS
Lower	15	13	
Depth of invasion			
Early[c]	12	5	NS
Advanced[d]	54	32	
Lymph node metastasis			
+	50	22	0.0836
–	16	15	
Lymphatic invasion			
+	60	36	NS
–	6	1	
Venous invasion			
+	58	33	NS
–	8	4	

[a]EBVnGC; EBV-negative GC.–[b]Location of tumor; upper/middle/lower third portion of the stomach. –[c]Tumor invasion within submucosa.–[d]Tumor invasion beyond muscularis propria.

PCR-single-strand conformational polymorphism analysis and loss of heterozygosity analysis of E-cadherin gene

Due to the amount of DNA available, only 11 out of the 15 EBVaGC cases examined in the immunohistochemical study were further subjected to PCR-single-strand conformational polymorphism (SSCP) and loss of heterozygosity (LOH) analyses. Exons 6–9 of *E-cadherin* gene were evaluated by PCR-SSCP analysis with subsequent sequencing of the abnormal bands. Exons 8 and 9 of the *E-cadherin* gene have been identified as the region of the mutation hot spot in diffuse-type gastric carcinoma.[29] PCR-SSCP analysis was performed according to the established protocols.[20,30] Electrophoresis was performed on 6% neutral polyacrylamide gels at 15 mA/1,500 V for 4 hr. The gels were dried and exposed to X-ray film at −80°C overnight. All experiments were performed in duplicate. MKN45, a cell line that harbors a mutation on exon 6, was used as a mutation-positive control.[30] When mobility shift SSCP bands were present, they were isolated from the gels and subjected to PCR using the same primer sets as those used in the prior PCR. The PCR products were cloned into the vector pCR II-TOPO (Invitrogen, Leek, The Netherlands). Sequencing was performed using a DYEnamic ET terminator cycle sequencing kit (Amersham Pharmacia Biotech, Uppsala, Sweden) with a DNA sequencer (Model 373A, Applied Biosystems).

The LOH study was performed using the tumor DNA and the matched DNA from the nonneoplastic mucosa. Radioactive PCR

TABLE II - PATHOLOGIC SIGNIFICANCE OF PROMOTER HYPERMETHYLATION OF *E-CADHERIN* IN EBV-ASSOCIATED GASTRIC CARCINOMA, AND DIFFUSE AND INTESTINAL SUBTYPES OF EBV-NEGATIVE GASTRIC CARCINOMA

	Frequencies of promoter hypermethylation						
	Total	Depth of invasion[a]			Lymph node metastasis		
		Early	Advanced	*p*	Negative	Positive	*p*
EBVaGC	95% (21/22)	100% (7/7)	94% (14/15)	NS	93% (14/15)	100% (7/7)	NS
EBVnGC diffuse[b]	65% (26/40)	100% (6/6)	59% (20/34)	0.0743	70% (7/10)	63% (19/30)	NS
EBVnGC intestinal[c]	46% (19/41)	29% (2/7)	50% (17/34)	NS	14% (2/14)	63% (17/27)	0.0038

[a]Early/advanced, tumor invasion within submucosa/tumor invasion beyond muscularis propria.–[b]EBV-negative GC showing diffuse type of histology. –[c]EBV-negative GC showing intestinal type of histology.

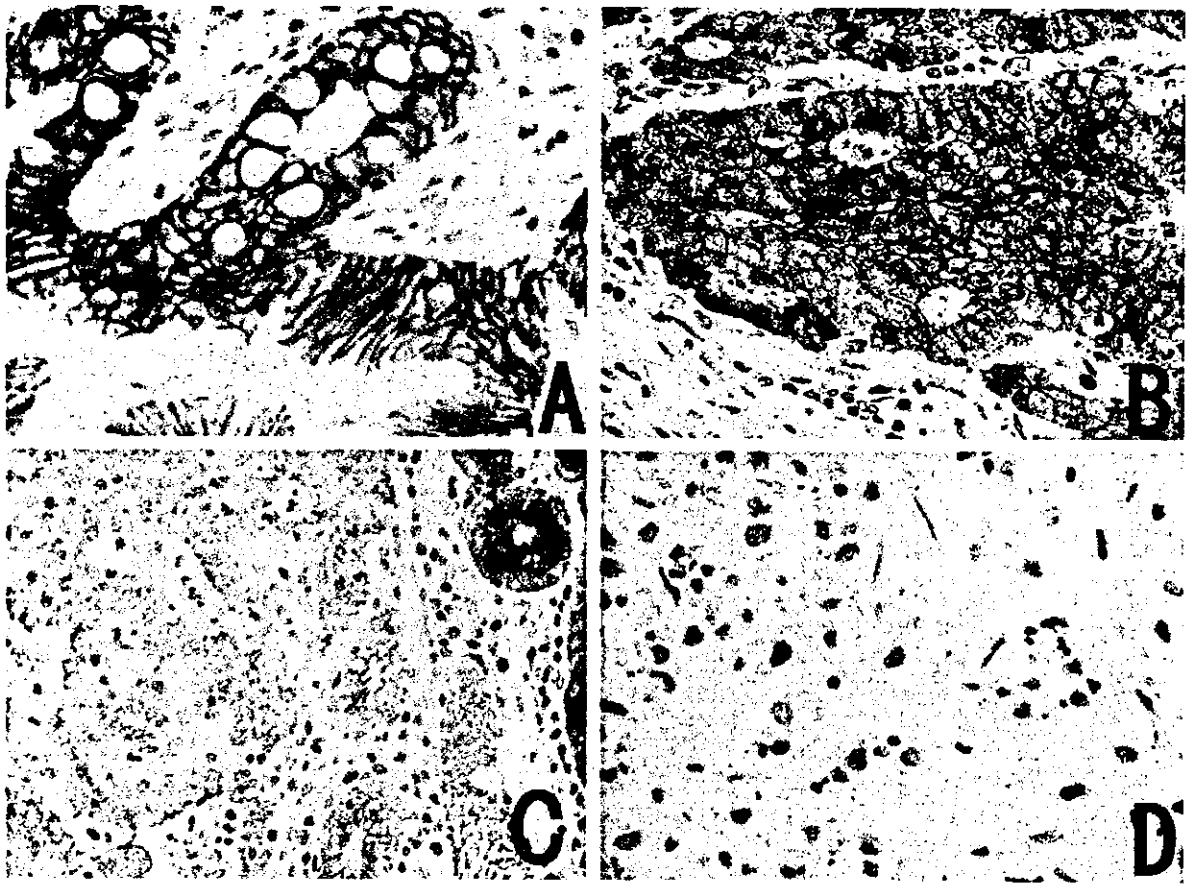

FIGURE 2 – Immunohistochemical staining pattern of E-cadherin in EBV-associated and EBV-negative gastric carcinoma. (*a*) Normal expression of E-cadherin in normal colonic mucosa. (*b*) Example of normal staining pattern in intestinal-type EBV-negative GC. (*c*) Heterogeneous staining pattern in EBVaGC. (*d*) Reduced staining pattern in diffuse-type EBV-negative GC. Original magnification × 400 for all panels.

amplification of microsatellite markers D16S265 and D16S301 was performed according to the procedures described by Machado *et al.*[19] PCR products were run in a 6% denaturing polyacrylamide gel with 5% crosslinking and exposed to X-ray film at room temperature overnight.

Regional heterogeneity of promoter hypermethylation of E-cadherin

Regional heterogeneity of promoter hypermethylation of *E-cadherin* was assessed in EBVaGC by the MSP analysis of the microdissected tumor tissue from the formalin-fixed, paraffin-embedded section. Two serial sections, 8 μm in thickness, were deparaffinized in xylene and rehydrated in alcohol. After the sections were briefly stained with hematoxyline, a 5 × 5 mm sized region was dissected from each with an 18 G needle tip. The tissue samples were treated with proteinase K (1 mg/ml) at 37°C overnight. After phenol-chloroform-isoamyl alcohol extraction and ethanol precipitation, each 1 μg of DNA was subjected to bisulfite modification as described above. Since the DNA was obtained from the formalin-fixed and paraffin-embedded sections, different primer sets were used to obtain shorter PCR products according the method of Herman *et al.*[25] The temperature profiles for the amplification were as follows: initial heating at 95°C for 5 min, 45 cycles of denaturation at 95°C for 45 sec, annealing at 57.0°C for

the methylated primer set and at 53.0°C for the unmethylated primer set and extension at 72°C for 45 sec, followed by a final extension at 72°C for 10 min.

Statistical analysis

Statistical analysis of the results was performed using the chi-square test or Fisher's exact test. Differences were considered to be significant at $p < 0.05$.

RESULTS

Promoter methylation of E-cadherin

Twenty-two cases of EBVaGC and 81 cases of EBV-negative GC were included in this study. The only significant difference between the 2 groups was the tumor location (cardia, gastric body in total cases: 22/22 in EBVaGC and 53/81 in EBV-negative GC).

The results of MSP analysis (Fig. 1) are presented in Table I. Nearly all of the carcinomas showed aberrant methylation of *E-cadherin* promoter in EBVaGC, and the frequency of this aberrant methylation was significantly higher in EBVaGC than in EBV-negative GC ($p = 0.0003$). The diffuse type of histology appeared to be correlated with the *E-cadherin* hypermethylation, albeit not to a statistically significant extent ($p = 0.0502$). Since 2/3 (15 of 22) of EBVaGC cases showed the diffuse type of histology, EBVaGC contributed to the relatively high frequency of aberrant methylation of *E-cadherin* in the diffuse type. Otherwise, the frequency of promoter hypermethylation did not differ significantly between any of the other groups classified by clinicopathologic factors such as age, gender, or location, depth of invasion and lymph node metastasis of the carcinoma.

Since E-cadherin is reported to relate to the histologic subtype of gastric carcinoma, EBV-negative GC was further divided into diffuse and intestinal types (Table II). The frequencies of aberrant methylation in these 2 subtypes of EBV-negative GC did not differ, and both were lower than the frequency in EBVaGC ($p = 0.0113$ and < 0.0001, respectively). However, the significance of the *E-cadherin* methylation appeared to be different in each subtype. When early and advanced stages were compared, the frequency of hypermethylation in the advanced stage (59%) was relatively lower than that in the early stage (100%) in the diffuse type of EBV-negative GC ($p = 0.0743$). On the other hand, the frequency of promoter hypermethylation increased as the tumor progressed from early (29%) to advanced carcinoma (50%) in the intestinal type of EBV-negative GC, albeit not to a statistically significant extent. The presence of lymph node metastasis was also found to be significantly correlated with promoter hypermethylation in this subtype of EBV-negative GC ($p = 0.0038$).

Immunohistochemistry of E-cadherin *and its correlation with promoter methylation*

Next, we investigated the expression of E-cadherin by immunohistochemistry in order to evaluate the correlation with promoter methylation. Both heterogeneous and reduced staining patterns were considered abnormal pattern (Fig. 2). Abnormal staining pattern was observed in 13 of 15 EBVaGC cases, 12 of 15 diffuse-type EBV-negative GC cases and 9 of 19 intestinal-type EBV-negative GC cases (Fig. 3). When the relationship between methylation status and immunohistochemical staining was analyzed in each subgroup, a significant correlation was noted only in the EBVaGC cases. On the other hand, significant number of the unmethylated cases showed abnormal staining pattern in the diffuse and intestinal types of EBV-negative GC cases.

Mutation and LOH of E-cadherin gene in EBVaGC

To exclude a possible contribution of genetic changes of *E-cadherin* in EBVaGC, PCR-SSCP was performed, and no mutation was observed in EBVaGC (Table III). MKN45 has 18 bp deletion at the exon 6-intron 6 boundary. At the experimental condition in the present study, the mutation of MKN45 was detected even when the percentage of MKN45 DNA was 10% in total DNA when mixed with DNA of nonneoplastic tissue. Similarly, LOH of *E-cadherin* was not observed in any of 11 cases examined (Table III).

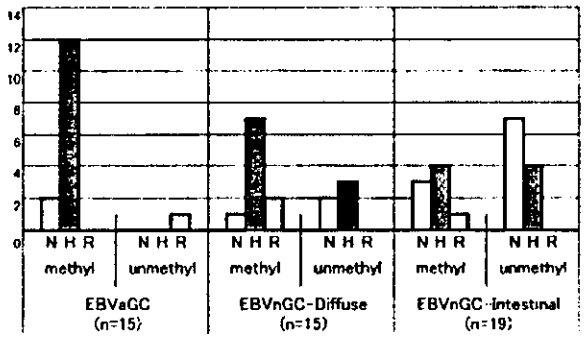

FIGURE 3 – Promoter methylation status and immunohistochemical staining patterns of E-cadherin in EBV-associated gastric carcinoma and diffuse and intestinal subtypes of EBV-negative gastric carcinoma. Twelve of 15 EBVaGC cases showed a heterogeneous staining pattern with promoter methylation, whereas this correlation was not observed in EBV-negative GC (EBVnGC). Methyl, methylated promoter; Unmethyl, unmethylated promoter; N, normal staining pattern; H, heterogeneous staining pattern; R, reduced staining pattern

Regional heterogeneity of promoter hypermethylation of E-cadherin in EBVaGC

To evaluate the regional heterogeneity of promoter hypermethylation of *E-cadherin* in EBVaGC, several samples were dissected from a section of each EBVaGC tumor (Table III). In 13 of 15 cases, the methylation status was successfully evaluated using the tissue samples of formalin-fixed and paraffin-embedded specimens (Table III). One of the cases evaluated did not show promoter methylation in the first evaluation using DNA derived from frozen tissue, but all of the cases showed methylation at least in one of the formalin-fixed samples. Heterogeneity of methylation status within the carcinoma was observed in all cases except 1 of 3 early carcinomas.

DISCUSSION

Epigenetic silencing of the gene expression by CpG island hypermethylation has been shown to play an important role in the carcinogenesis of various organs, including the stomach.[31–33] In recent investigations of EBVaGC cases, Kang *et al.*[9] and our own group[10] observed high frequencies of promoter methylation in various cancer-related genes such as *p14, p15, p16, DAPK, GSTP, TIMP-3* and *E-cadherin*, but not in *hMLH1* and *MGMT*. This finding suggests that a global but selective DNA hypermethylation of the cellular genes may occur in the EBV-infected epithelial cells. In the present study focusing on the E-cadherin protein of the stomach, we confirmed on a larger scale that nearly all of the carcinoma tissues of EBVaGC showed CpG island methylation of *E-cadherin*. Furthermore, we demonstrated that abnormal expression occurred in nearly all of EBVaGC cases, while such a correlation was not strictly observed in EBV-negative GC. Since neither mutation nor LOH was observed in EBVaGC, epigenetic silencing is a major mechanism of E-cadherin dysfunction in EBVaGC.

Most of the cases with hypermethylation in the present study showed a heterogeneous staining pattern rather than the reduced type in EBVaGC. This was consistent with our findings from earlier immunohistochemistry studies on p16 showing a marked decrease of p16 expression rather than a total loss of expression. Current studies on gene regulation by promoter methylation fit well with these findings. In cell lines from the human bladder, colon cancers and melanoma, Bender *et al.*[34] found that the ex-

TABLE III - EVALUATION OF MUTATION, LOH AND REGIONAL HETEROGENEITY OF PROMOTER HYPERMETHYLATION OF *E-CADHERIN* IN EBV-ASSOCIATED GASTRIC CARCINOMAS

	Case	Age	Gender	Histology	Depth[a]	Mutation[b]	LOH[c]	Methylation in frozen section[d]	Methyl[e]/sample[f]
1	J84	43	M	Diffuse	Early	–	–	+	1/3
2	F239	65	M	Diffuse	Early	–	–	+	1/2
3	J49	45	M	Intestinal	Early	–	–	+	3/3
4	F190	73	F	Diffuse	Advanced	ND	ND	+	1/4
5	F187	67	M	Diffuse	Advanced	ND	ND	+	2/5
6	F159	66	F	Diffuse	Advanced	–	–	+	1/5
7	F108	80	M	Diffuse	Advanced	–	–	+	1/3
8	F284	50	M	Diffuse	Advanced	–	–	+	1/3
9	F72	65	M	Diffuse	Advanced	–	–	+	2/4
10	F169	54	M	Diffuse	Advanced	ND	ND	–	1/3
11	J1	22	F	Intestinal	Advanced	–	–	+	1/4
12	F197	73	F	Intestinal	Advanced	ND	ND	+	1/3
13	J183	60	M	Intestinal	Advanced	–	–	+	3/5
14	F287	75	M	Intestinal	Advanced	–	–	+	Failed[g]
15	J150	62	M	Intestinal	Advanced	–	–	+	Failed[g]
16	J243	37	M	Intestinal	Early	ND	ND	+	ND
17	F196	65	M	Diffuse	Advanced	ND	ND	+	ND
18	F273	69	M	Diffuse	Advanced	ND	ND	+	ND
19	F63	34	M	Diffuse	Advanced	ND	ND	+	ND
20	F85	61	M	Diffuse	Advanced	ND	ND	+	ND
21	J355	62	M	Diffuse	Advanced	ND	ND	+	ND
22	J360	83	F	Diffuse	Advanced	ND	ND	+	ND

[a]Early/advanced, tumor invasion within submucosa/tumor invasion beyond muscularis propria.–[b]Result of mutation analysis by PCR-SSCP; –; no mutation was detected; ND, not done. –[c]–, no LOH was detected.–[d]+, methylated; –, unmethylated. –[e]Number of samples that showed promoter hypermethylation.–[f]Number of samples obtained from one tumor by microdissection. –[g]MSP was not successful.

pression of p16 is highly affected by the frequency of methylation of the *p16* promoter, but not by the presence of the methylation itself. Our study of the microdissection confirmed heterogeneity in the methylation status within each tumor. There are 2 explanations for this heterogeneity: hypermethylation occurs in a subpopulation of the carcinoma. Alternatively, the maintenance of hypermethylation is considerably disturbed in the progression of the carcinoma,[35,36] even though hypermethylation occurs in a uniform manner at early stage of cancer development. Methylation was observed in nearly all of the cases of EBVaGC, and the case showing methylation in all of the samples was the early gastric carcinoma in the present study. Thus, the latter possibility would constitute the most likely mechanism in EBVaGC.

As for the discrepancy between promoter methylation and gene expression in EBV-negative GC, regional heterogeneity of promoter methylation might exert in the cases of positive methylation but normal expression. On the other hand, in the cases of negative methylation but abnormal expression, at least 3 mechanisms[37] are possible: gene mutation,[18,30] posttranslational truncation or modification[38] and transcriptional repressor.[38–41] Thus, other than EBVaGC, further studies are necessary to disclose the regulation of *E-cadherin* gene expression in GC.

As an additional result, the present study provides some detailed statistical insights into the correlation between promoter methylation, gene expression/localization, tumor stages and tumor type in EBV-negative GC. In the intestinal-type EBV-negative GC, promoter hypermethylation of *E-cadherin* was correlated with both lymph node metastasis and invasion beyond the muscular layer. Since promoter methylation was not faithfully reflected in overall gene expression, promoter-methylated subpopulation within the tumor may play a primary role in the progression of this type of gastric carcinoma. On the other hand, the frequency of hypermethylation decreased from 100% to 59% as the carcinomas progressed from early to advanced in diffuse type. The maintenance of hypermethylation may be considerably disturbed in the progression of the carcinoma of the diffuse type of EBV-negative GC, as in the case of EBVaGC.

In conclusion, in addition to p16, the abnormality of E-cadherin expression caused by the aberrant methylation of *E-cadherin* gene promoter is closely associated with the development of EBVaGC. As the significance of aberrant methylation of *E-cadherin* differs between EBVaGC and EBV-negative GC, we can conclude that the recognition of this type of gastric carcinoma is critical for the evaluation of carcinogenesis of the stomach.

REFERENCES

1. Fukayama M, Chong JM, Kaizaki Y. Epstein-Barr virus and gastric carcinoma. Gastric Cancer 1998;1:104–14.
2. Fukayama M, Chong JM, Uozaki H. Pathology and molecular pathology of Epstein-Barr virus-associated gastric carcinoma. In: Takada K, editor. Epstein-Barr virus and human cancer. Berlin: Springer-Verlag, 2001. 91–102.
3. Fukayama M, Hayashi Y, Iwasaki Y, Chong JM, Ooba T, Takizawa T, Koike M, Mizutani S, Miyaki M, Hirai K. Epstein-Barr virus-associated gastric carcinoma and Epstein-Barr virus infection of the stomach. Lab Invest 1994;7:73–81.
4. Chong JM, Sakuma K, Sudo M, Osawa T, Ohara E, Uozaki H, Shibahara J, Kuroiwa K, Tominaga S, Hippo Y, Aburatani H, Funata N, et al. Interleukin1β expression in human gastric carcinoma with Epstein-Barr virus infection. J Virol 2002;76:6825–31.
5. Chong JM, Fukayama M, Hayashi Y, Funata N, Takizawa T, Koike M, Muraoka M, Kikuchi-Yanoshita M, Mizuno S. Expression of CD44 variants in gastric carcinoma with or without Epstein-Barr virus. Int J cancer 1997;74:450–4.
6. Sugiura M, Imai S, Tokunaga M, Koizumi S, Uchizawa M, Okamoto K, Osato T. Transcriptional analysis of the Epstein-Barr virus gene expression in EBV-positive gastric carcinoma: unique viral latency in the tumor cells. Br J Cancer 1996;74:625–31.
7. zur Hausen A, Brink AATP, Craanen ME, Middeldrop JM, Meijer CJLM, van den Brule AJC. Unique transcription pattern of Epstein-Barr virus (EBV) in EBV-carrying gastric adenocarcinomas: expression of the transforming BARF1 gene. Cancer Res 2000;60:2745–8.
8. Chong JM, Fukayama M, Hayashi Y, Takizawa T, Koike M, Konishi M, Kikuchi-Yanoshita R, Miyaki M. Microsatellite instability in the progression of gastric carcinoma. Cancer Res 1994;54:4595–7.
9. Kang GH, Lee S, Kim WH, Lee HW, Kim JC, Rhyu MG, Ro JY. Epstein-Barr virus-positive gastric carcinoma demonstrates frequent aberrant methylation of multiple genes and constitutes CpG island methylator phenotype-positive gastric carcinoma. Am J Pathol 2002; 160:787–94.
10. Chong JM, Sakuma K, Sudo M, Ushiku T, Uozaki H, Shibahara J, Nagai H, Funata N, Taniguchi H, Aburatani H, Fukayama M. Global

and non-random CpG-island methylation in gastric crcinoma associated with Epstein-Barr virus. Cancer Sci 2003;94:76–80.
11. Osawa T, Chong JM, Sudo M, Sakuma K, Uozaki H, Shibahara J, Nagai H, Funata N, Fukayama M. Reduced expression and promoter methylation of *p16* gene in Epstein-Barr virus-associated gastric carcinoma. Jpn J Cancer Res 2002;93:1195–200.
12. Takeichi M. Morphogenetic roles of classic cadherins. Cur Opin Cell Biol 1995;7:619–27.
13. Takeichi M. Cadherin cell adhesion receptors as morphogenetic regulator. Science 1991;251:1451–5.
14. Bracke ME, van Roy FM, Mareel MM. The E-cadherin/catenin complex in invasion and metastasis. In: Gunther U, Birchmeier W, eds. Attempts to understand metastasis formation. Berlin: Springer-Verlag, 1996. 123–61.
15. Shino Y, Watanabe A, Yamada Y, Tanase M, Yamada T, Matsuda M, Yamashita J, Tatsumi M, Miwa T, Nakano H. Clinicopathologic evaluation of immunohistochemical E-cadherin expression in human gastric carcinomas. Cancer 1995;76:2193–201.
16. Shun CT, Wu MS, Lin JT, Wang HP, Houng RL, Lee WJ, Wang TH, Chuang SM. An immunohistochemical study of E-cadherin expression with correlations to clinicopathological features in gastric cancer. Hepato-Gastroenterology 1998;45:944–9.
17. Oka H, Shiozaki H, Kobayashi K, Tahara H, Tamura S, Miyata M, Doki Y, Iihara K, Matsuyoshi N, Hirano S, Takeichi M, Mori T. Immunohistochemical evaluation of E-cadherin adhesion molecule expression in human gastric cancer. Virchows Arch 1992;421:149–56.
18. Becker KF, Atkinson NJ, Reich U, Becker I, Nekarda H, Siewert JR, Hofler H. *E-cadherin* gene mutations provide clues to diffuse type gastric carcinomas. Cancer Res 1994;54:3845–52.
19. Machado JC, Soares P, Carneiro F, Rocha A, Beck S, Blin N, Berx G, Sobrinho-Simoes M. *E-cadherin* gene mutations provide a genetic basis of the phenotypic divergence of mixed gastric carcinomas. Lab Invest 1999;79:459–65.
20. Tamura G, Sakata K, Nishizuka S, Maesawa C, Suzuki Y, Iwaya T, Terashima M, Saito K, Satodate R. Inactivation of the *E-cadherin* gene in primary gastric carcinomas and gastric carcinoma cell lines. Jpn J Cancer Res 1996;87:1153–9.
21. Guilford P, Hopkins J, Harraway J, McLeod M, McLeod N, Harawira P, Taite H, Scoular R, Miller A, Reeve AE. E-cadherin germline mutations in familial gastric cancer. Nature 1998;392:402–5.
22. Wu MS, Shun CT, Wu CC, Hsu TY, Lin MT, Chang MC, Wang HP, Lin JT. Epstein-Barr virus-associated gastric carcinomas: relation to *H. pylori* infection and genetic alterations. Gastroenterology 2000; 118:1031–8.
23. Japanese Gastric Cancer Association. Japanese classification of gastric carcinoma: 2nd English edition. Gastric Cancer 1998;1:10–24.
24. Lauren P. The two histological main types of gastric carcinoma, diffuse and so-called intestinal-type carcinoma. Acta Pathol Microbiol Scand 1965;64:31–49.
25. Herman JG, Graff JR, Myohanen S, Nelkin BD, Baylin SB. Methylation-specific PCR: a novel PCR assay for methylation status of CpGislands. Proc Natl Acad Sci 1996;93:9821–6.
26. Kallakury BVS, Sheehan CE, Winn-Deen E, Oliver J, Fisher HAG, Kaufman RP, Ross JS. Decreased expression of catenins (α and β), p120 CTN, and E-cadherin cell adhesion proteins and *E-cadherin* gene promoter methylation in prostatic adenocarcinomas. Cancer 2001;92:2786–95.
27. Shimoyama Y, Hirohashi S. Expression of E- and P-cadherin in gastric carcinomas. Cancer Res 1991;51:2185–92.
28. Jawhari A, Jordan S, Poole S, Browne P, Pignatelli M, Farthing MJG. Abnormal immunoreactivity of the E-cadherin-catenin complex in gastric carcinoma: relationship with patient survival. Gastroenterology 1997;112:46–54.
29. Berx G, Becker KF, Hofler H, van Roy F. Mutations of the human E-cadherin (CDH1) gene. Hum Mutat 1998;12:226–37.
30. Oda T, Kanai Y, Oyama T, Yoshiura K, Shimoyama Y, Birchmeier W, Sugimura T, Hirohashi S. *E-cadherin* gene mutations in human gastric carcinoma cell lines. Proc Natl Acad Sci 1994;91:1858–62.
31. Tamura G, Yin J, Wang S, Fleisher AS, Zou TT, Abraham JM, Kong DH, Smolinski KN, Wilson KT, James SP, Silverberg SG, Nishizuka S, et al. *E-cadherin* gene promoter hypermethylation in gastric carcinomas. J Natl Cancer I 2000;92:569–73.
32. Machado JC, Oliveira C, Carvalho R, Soares P, Berx G, Caldas C, Seruca R, Carneiro F, Sobrinho-Simoes M. *E-cadherin* gene (CDH1) promoter methylation as the second hit in sporadic diffuse gastric carcinoma. Oncogene 2001;20:1525–8.
33. Oue N, Motoshita J, Yokozaki H, Hayashi K, Tahara E, Taniyama K, Matsusaki K, Yasui W. Distinct promoter hypermethylation of p16(INK4a), CDH1, and RAR-beta in intestinal, diffuse-adherent, and diffuse-scattered type gastric carcinomas. J Pathol 2002;198:55–9.
34. Bender CM, Pao MM, Jones PA. Inhibition of DNA methylation by 5-aza-2′-deoxycytidine suppresses the growth of human tumor cell lines. Cancer Res 1998;58:95–101.
35. Joo YE, Rew JS, Kim HS, Choi SK, Park CS, Kim SJ. Changes in the E-cadherin-catenin complex expression in early and advanced gastric cancers. Digestion 2001;64:111–9.
36. Graff JR, Gabrielson E, Fujii H, Baylin SB, Herman JG. Methylation patterns of the E-cadherin 5′ CpG island are unstable and reflect the dynamic, heterogenous loss of E-cadherin expression during metastatic progression. J Biol Chem 2000;275:2727–32.
37. Rosivatz E, Becker I, Specht K, Fricke E, Luber B, Busch R, Hofler H, Becker KF. Differential expression of the epithelial-mesenchymal transition regulators Snail, SIP1, and Twist in gastric cancer. Am J Pathol 2002;161:1881–91.
38. Rashid MG, Sanda MG, Vallorosi CJ, Rios-Doria J, Rubin MA, Day ML. Posttranslational truncation and inactivation of human E-cadherin distinguishes prostate cancer from matched normal prostate. Cancer Res 2001;61:489–92.
39. Cano A, Perez-Moreno MA, Rodrigo I, Locascio A, Blanco MJ, del Barrio MG, Portillo F, Nieto MA. The transcription factor Snail controls epithelial-mesenchymal transitions by repressing E-cadherin expression. Nat Cell Biol 2000;2:76–83.
40. Batlle E, Sancho E, Franci C, Dominguez D, Monfar M, Baulida J, de Herreros AG. The transcription factor Snail is a repressor of *E-cadherin* gene expression in epithelial tumour cells. Nat Cell Biol 2000;2:84–9.
41. Comijn J, Berx G, Vermassen P, Verschueren K, van Grunsven L, Bruyneel E, Mareel M, Huylebroeck D, van Roy F. The two-handed E box binding zinc finger protein SIP1 down regulates E-cadherin and induces invasion. Mol Cell 2001;7:1267–78.

[CANCER RESEARCH 64, 7263–7270, October 15, 2004]

Distinct Chromosomal Bias of Gene Expression Signatures in the Progression of Hepatocellular Carcinoma

Yutaka Midorikawa,[1,3] Shuichi Tsutsumi,[1] Kunihiro Nishimura,[2] Naoko Kamimura,[1] Makoto Kano,[2] Hirohiko Sakamoto,[4] Masatoshi Makuuchi,[3] and Hiroyuki Aburatani[1]

[1]Genome Science Division, [2]Intelligent Cooperative Systems Division, Research Center for Advanced Science and Technology, and [3]Hepato-Biliary-Pancreatic Surgery Division, The University of Tokyo, Tokyo; and [4]Department of Surgery, Saitama Cancer Center, Saitama, Japan

ABSTRACT

To identify the chromosomal aberrations associated with the progression of liver cancer, we applied expression imbalance map analysis to gene expression data from 31 hepatocellular carcinomas and 19 noncancerous tissues. Expression imbalance map analysis, which detects mRNA expression imbalance correlated with chromosomal regions, showed that expression gains of 1q21-23 (74%), 8q13-21 (48%), 12q23-24 (41%), 17q12-21(48%), 17q25 (25%), and 20q11 (22%) and losses of 4q13 (48%), 8p12-21 (32%), 13q14 (32%), and 17p13 (29%) were significantly associated with hepatocellular carcinoma. Most regions with altered expression identified by expression imbalance map were also identified in previous reports using comparative genomic hybridization. We demonstrated chromosomal copy number gain in 1q21-23 and loss in 17p13 by genomic quantitative PCR, suggesting that gene expression profiles reflect chromosomal alterations. Furthermore, expression imbalance map analysis revealed that more poorly differentiated hepatocellular carcinoma contain more chromosomal alterations, which are accumulated in a stepwise manner in the course of hepatocellular carcinoma progression: expression imbalance of 1q, 8p, 8q, and 17p occur as early events in hepatocarcinogenesis, and 12q, 17q25 and 20q occur as later events. In particular, expression gain of 17q12-21 and loss of 4q were seen to accumulate constantly through the dedifferentiation process. Our data suggest that gene expression profiles are subject to chromosomal bias and that expression imbalance map can correlate gene expression to gene loci with high resolution and sensitivity.

INTRODUCTION

Hepatocellular carcinoma develops with dedifferentiation after liver injury by chronic hepatitis viral infection. In multistep hepatocarcinogenesis, several molecular events accumulate in a fashion that parallels the clinical progression of liver cancer (1, 2). Some studies have tried to identify the genes altered in dedifferentiation of hepatocellular carcinoma using samples with a nodule-in-nodule appearance (2, 3). Still, little is known about the genes that play a pivotal role during the course of liver cancer progression.

Genomic amplification of oncogenes and inactivation of tumor suppressor genes are frequently associated with cancer progression. Comparative genomic hybridization (CGH) has contributed to our basic cancer understanding and diagnosis of cancer (4) but can only detect genomic alterations > 20 Mb. This low resolution makes it difficult for CGH to identify genes differentially expressed in carcinogenesis. To detect amplification events involving small genomic regions, high-resolution analysis of DNA copy number variation using cDNA microarrays has been used (5–7). However, because this technology only analyzes genomic DNA, supplementary experiments are required to confirm the expression of candidate genes in tumorigenesis. Microarrays have also been used to obtain comprehensive measurements of genome-wide expression profiles. Using such techniques, classification of cancer specimens or identification of gene sets for carcinogenesis and cancer progression have been reported by many researchers (2, 8–11).

Information about genome dosage and transcriptome may be obtained through microarray technologies if gene expression and gene localization data are integrated. In our study of oligodendroglioma, we showed that biological differences between genetic subsets of oligodendroglioma are reflected in their gene expression profiles and that genomic copy number alteration consistently accompanies perturbation of the transcriptome (12). Similarly, Virtaneva *et al.* (13) demonstrated an association between trisomy 8 and overexpression of genes on chromosome 8 in acute myeloid leukemia, and Tay *et al.* (11) performed CGH and expression microarray using gastric cancer specimens integrating CGH data with the microarray results.

Recently, based on mRNA expression, we have reported a method for constructing a transcriptome map (14). The expression imbalance map is a visualization method for detecting expression imbalance in regions of chromosomes. It extends beyond simple spatial mapping of microarray expression profiles on chromosomal locations to profile genomic losses and gains at a much higher resolution than CGH. In the expression imbalance map, signal noise can be reduced using a moving average compared with conventional methods, and users can determine thresholds. Furthermore, the expression imbalance map not only detects the expression imbalance frequency across all cases but also detects individual differences between cancer specimens. In addition, the expression imbalance map allows observation of both expression imbalance and the expression of each gene simultaneously. We previously applied the expression imbalance map to gene expression data derived from squamous cell lung carcinoma and detected, as regional signal images, several novel and many known loci with frequent genomic losses or gains on various chromosomes (14).

In the present study, we have focused on chromosomal bias in transcripts during multistep hepatocarcinogenesis. We applied the expression imbalance map method to gene expression data of hepatocellular carcinoma and observed a stepwise change of expression along at defined chromosomal loci in liver cancer progression. Genomic quantitative PCR (qPCR) analysis confirmed that expression imbalance map data correlated with genomic aberrations. The novel regions identified by the expression imbalance map may play pivotal roles during the course of dedifferentiation of hepatocellular carcinoma and likely contain some candidate genes responsible for liver cancer progression.

MATERIALS AND METHODS

Patients and Tissue Samples. Thirty-one patients with hepatocellular carcinoma undergoing hepatectomy in the Hepato-Biliary-Pancreatic Surgery Division, Department of Surgery, Graduate School of Medicine, University of

Received 4/17/04; revised 8/3/04; accepted 8/10/04.

Grant support: Grant-in-Aid for Scientific Research (B) 12557051 and 13470114 and Scientific Research on Priority Areas (C) 12217031 from The Ministry of Education, Science, Sports and Culture (H. Aburatani), Health and Labor Sciences Research Grants on Hepatitis and BSE and The Mitsubishi Foundation (H. Aburatani), and Mitsui Life Social Welfare Foundation (Y. Midorikawa).

The costs of publication of this article were defrayed in part by the payment of page charges. This article must therefore be hereby marked *advertisement* in accordance with 18 U.S.C. Section 1734 solely to indicate this fact.

Requests for reprints: Hiroyuki Aburatani, Genome Science Division, Research Center for Advanced Science and Technology, The University of Tokyo, 4-6-1 Komaba, Meguro-ku, Tokyo 153-8904, Japan. Phone: 81-3-5452-5352; Fax: 81-3-5452-5355; E-mail: haburata-tky@umin.ac.jp.

Tokyo, or the Department of Surgery, Saitama Cancer Center, were included in this study with informed consent. Among the 31 patients with hepatocellular carcinoma, 10 were positive for hepatitis B surface antigen and 21 for hepatitis C viral antibody. GeneChip analysis was performed using 50 samples, including 31 hepatocellular carcinomas and 19 surrounding noncancerous tissues. Clinical factors and tumor status based on histologic findings of resected specimens are summarized in Table 1.

The surgical specimens were immediately cut into small pieces after resection, snap frozen in liquid nitrogen and stored at −80°C.

RNA Extraction and Oligonucleotide Microarray. Total RNA was isolated from frozen tissue using Isogene (Nippon Gene, Tokyo, Japan), according to the manufacturer's protocol. Experimental procedures for GeneChip were performed according to GeneChip Expression Analysis Technical Manual (Affymetrix, Santa Clara, CA), using 15 μg of total RNA. Samples were analyzed on U95A array chips (Affymetrix).

Normalization and Filtering of Intensity of Gene Expression. Before analysis, we normalized and filtered the raw data. A quantile normalization procedure was used for the probe intensity distribution across different chips. The average of expression level intensity, the average difference, was scaled to 100, and for each expression data set, where the average difference values lay outside the range (1 to 10,000), the values was reset to a minimum 1 and to a maximum of 10,000. Genes where the coefficient of variation through all of the samples was <0.3 were excluded from analysis. Subsequently, all values were log-transformed for additional analysis.

Expression Imbalance Map. The expression imbalance map was applied to gene expression data of hepatocellular carcinoma and noncancerous tissues obtained by microarray. Gene locus information was obtained from the web sites for Genes On Sequence Map (*Homo sapiens* build 33). The basic concept and method of expression imbalance map are described elsewhere (14). Briefly, gene expression levels of cancer specimens were compared with the average of noncancerous tissues, and the regions in which the numbers of up-regulated or down-regulated genes were significantly concentrated were mapped on the chromosomal region and constitute an expression imbalance map.

Table 1 *Clinical factors and tumor status based on histologic findings of resected specimens*

Sample no.	Age (y)	Gender	Hepatitis virus	Differentiated grade	Tumor size (mm)	fc	sf	vv	vp	b	im	s
w1	48	M	HB	WD	22	−	+	−	−	−	−	−
w2	72	F	HC	WD	33	−	+	−	−	−	−	−
w3	62	M	HB	WD	31	−	+	−	−	−	−	−
w4	66	F	HC	WD	40	−	+	−	−	−	−	−
w5	65	M	HC	WD	27	+	+	−	−	−	−	−
w6	75	M	HC	WD	40	+	+	−	−	−	−	−
w7	68	F	HB	WD	10	−	−	−	−	−	−	−
w8	60	M	HC	WD	14	−	−	−	−	−	−	−
w9	66	M	HC	WD	36	+	−	−	+	+	+	−
w10	66	M	HC	WD	48	+	−	−	−	−	+	−
m1	69	F	HB	MD	38	+	−	−	−	−	−	−
m2	71	M	HC	MD	15	−	+	−	−	−	−	−
m3	47	M	HB	MD	24	+	+	−	+	+	−	−
m4	71	F	HC	MD	22	−	+	−	−	−	−	−
m5	71	F	HC	MD	30	+	+	−	−	−	−	+
m6	69	M	HC	MD	50	+	+	−	−	−	−	−
m7	70	F	HC	MD	23	−	+	−	−	−	−	−
m8	53	M	HB	MD	45	+	+	−	−	−	−	−
m9	63	F	HC	MD	20	+	+	−	−	−	−	−
m10	50	M	HB	MD	25	−	+	−	+	−	−	−
m11	70	M	HC	MD	20	+	−	−	−	−	−	−
m12	49	M	HB	MD	22	−	+	−	+	−	+	−
m13	62	M	HC	MD	50	+	+	−	−	−	−	−
p1	54	M	HB	PD	11	−	+	−	−	−	−	−
p2	65	M	HC	PD	35	+	−	−	−	−	+	+
p3	56	F	HB	PD	45	−	−	−	−	−	−	+
p4	70	F	HC	PD	30	−	−	+	−	−	−	−
p5	63	M	HC	PD	40	+	+	−	−	−	−	−
p6	72	M	HC	PD	110	−	−	−	−	−	−	+
p7	70	M	HC	PD	45	+	−	−	−	−	−	−
p8	60	M	HC	PD	85	+	+	−	+	+	+	−

Abbreviations: fc, capsule formation; sf, septum formation; vv, tumor thrombus in hepatic vein; vp, tumor thrombus in portal vein; b, tumor thrombus in bile duct; im, intrahepatic metastasis; s, serosal invasion; M, male; F, female; HB, hepatitis B virus infection; HC, hepatitis C virus infection; WD, well differentiated HCC; MD, moderately differentiated HCC, PD; poorly differentiated HCC.

On the basis of the statistical probability, P, of rank sum, the differential level E value was defined as follows: $E = -\log_{10}P$.

The chromosomal regions with expression gain or loss were defined according to both E value and range of alteration of gene expression.

Clustering Hepatocellular Carcinoma Samples Using Chromosomal Regions with Expression Imbalance. A heat map was constructed using expression imbalance map-positive chromosomal regions as binary variables. Hepatocellular carcinoma samples were arranged in order of the total number of positive regions, and the samples with less than two positive regions were defined as group1, three or four positive regions as group 2, and more than five positive regions as group3. Next, considering the length of positive regions, expression imbalance in each 100-kb region was calculated, and the sum of the length of positive chromosomal change in each sample was displayed graphically as the intensity of red or blue. Thirty-one tumor samples were arranged in accordance to tumor differentiation grade, and the total length of transcriptome alterations in each sample were compared by ANOVA.

DNA Extraction and qPCR. Genomic DNA was extracted from fresh-frozen tissue, using the QIAamp DNA Mini kit (Qiagen, Valencia, CA), according to the manufacturer's instructions. PCR amplification was performed using Taq Polymerase and 20 ng of sample DNA. Oligonucleotide primers were designed to amplify genomic DNA fragments near the chromosomal locus of 1q21-23, encoding *CCT3* (145 bp), *PSMB4* (115 bp), 12q23-24, encoding *CKAP4* (141 bp), *UNG* (140 bp), 17p13, encoding *ASGR1* (136 bp), *DKFZP566H073* (168 bp), and β-actin (132 bp) as a control reference. The primers used were as follows: *CCT3*, 5′-TGACATCGTTTCAGGCCAC-3′ and 5′-GCACTCTGGCTCAGGAAAAG-3′; *PSMB4*, 5′-TGGCTCGTTTCCGCAACATC-3′ and 5′-ACCATCTGGCCGAGAACTTG-3′; *CKAP4*, 5′-GTGCAGTCTTTGCAAGCCAC-3′ and 5′-CTGGAGTTTCTGCAGCACTTC-3′; *UNG*, 5′-TGCTTAGAAAGGTCCCCTTG-3′ and 5′-GGCCAGATTCTGGAAAGTTG-3′; *ASGR1*, 5′-TCCACGTGAATCTGCACCTC-3′ and 5′-GAGCTCAGCTGCTGGATATC-3′; *DKFZP566H073*, 5′-AGACCTGCCCCATTTGCAAG-3′ and 5′-CAAAGGAGGTGGGAAGAGTG-3′; and β-actin, 5′-GACCTGACTGACTACCTCATG-3′ and 5′-CATCTCTTGCTCGAAGTCCAG-3′. qPCR for detecting gain of chromosome 1q21-23 and 12q23-24 and loss of chromosome 17p13 were performed using an iCycler (Bio-Rad, Hercules, CA). The relative quantification is given by the ratio between the mean value of the target gene and the mean value of β-actin in each sample.

RESULTS

Expression Imbalance Map for Detecting Expression Imbalance Regions. The expression imbalance map was applied to 31 hepatocellular carcinomas, comparing their expression data to the average of expression across 19 noncancerous tissues (Fig. 1*A*). Various criteria may be used to define expression imbalance regions. When expression imbalance regions were defined as those with E values > 2 and a region of >3.0Mb, compared with the background liver, expression gains on chromosome arms of hepatocellular carcinoma were observed on 1q21-23 (74%), 8q13-21 (48%), 12q23-24 (41%), 17q12-21 (48%), 17q25 (25%), and 20q11 (22%) and expression losses were detected on 4q13 (48%), 8p12-21(32%), 13q14 (32%), and 17p13 (29%; Fig. 1, *B* and *C*). To provide a comparison between our data and previously reported observations of chromosomal alterations of hepatocellular carcinoma obtained by CGH, chromosomal arms with expression gain or loss are summarized in Table 2. Most regions with altered expression, as determined by the expression imbalance map, were also indicated in previous reports using CGH. Notable exceptions are a gain of 12q, which has never been reported previously, and a loss of 16q, which has been demonstrated in many previous reports, but was not identified in our analysis.

Gene list of the imbalanced region is shown with their median and average signal intensities and SDs in the tumors and controls (Supplemental Fig. 1).[5]

Comparison with existing CGH data sets for hepatocellular carci-

[5] Internet address: http://www2.genome.rcast.u-tokyo.ac.jp/hcc.

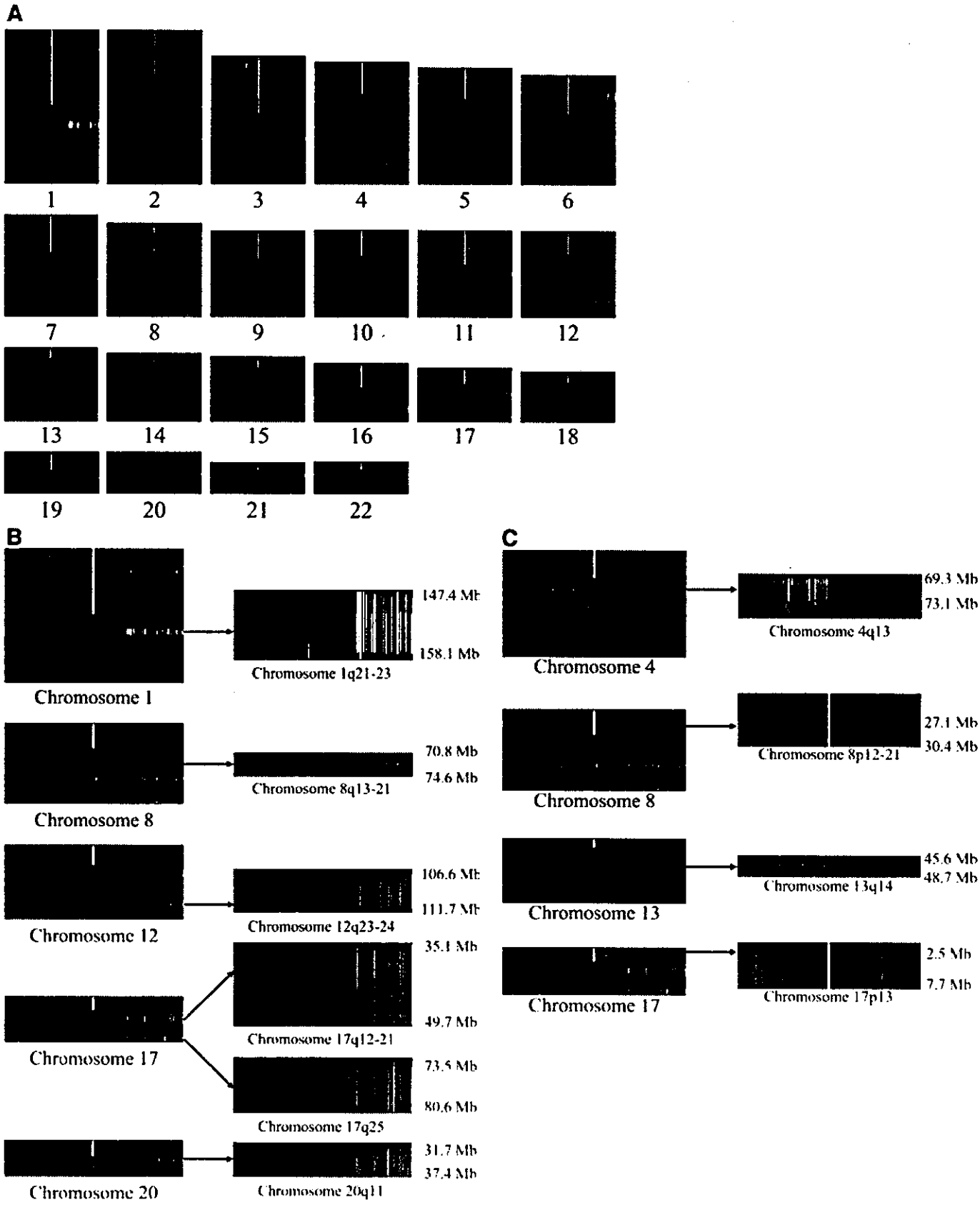

Fig. 1. Expression imbalance map for detecting expression imbalance regions in hepatocellular carcinoma. *A*. Regions of under- and overexpression in hepatocellular carcinoma were visualized on the *left side* and the *right side*, respectively, as gray regional signals. Each column represents tissue samples. The lighter areas correspond to higher probability of an expression imbalance region. The expression imbalance map enables the user to identify many more genes by referring to the more expanded area with lower luminance. This figure shows the expression imbalance at an E value > 2. *B*, expression imbalance region at an E value > 2 and a range of expression gain > 3.0 Mb. The length assigned to each chromosome is proportional to the number of Locus IDs on the chromosome. *C*, expression imbalance region at E value > 2 and a range of expression loss > 3.0 Mb.

Table 2 *Expression imbalance region and chromosomal alteration in hepatocellular carcinoma*

EIM		Others by CGH								
Chromosome		(16)	(18)	(19)	(20)	(23)	(25)	(26)	(27)	(28)
Gains										
1q	74	86	57	77	73	66	72	46	58	78
5p					38					
6p								20	33	
7q					40					
8q	48	77	52	52	83	48	48	31	60	66
11q				26						
12q	41									
17q	48		29				30	43	33	
20q	22		29			20	37			
xq					50					
Losses										
1p						36		37		
4q	48	59	33	35	40	40	43	48	70	32
5q								35		
6q			19					23	37	
8p	35	77		26	44	32	37	28	65	29
10q										17
13q	32		19	55			37	20	37	37
16p					46					
16q		50	14	52	63	70	30	33	54	46
17p	29			52	60	52		37	51	51
19p						42				
22q						28				

Expression gain or loss region by EIM was defined as E value > 2 and the range > 3.0 Mb. Figure means percentage of positive region. The number in parenthesis corresponds with reference number.

Abbreviation: EIM, expression imbalance map.

noma suggests that gene expression profiles reflect chromosomal alterations and that the expression imbalance map is a useful tool for estimating chromosomal change from expression data.

Classification of Hepatocellular Carcinomas by Chromosomal Bias of Gene Expression. Expression imbalance map analysis showed that genes with expression change are derived from particular chromosomal regions with altered copy number. To identify possible association between these chromosomal alterations and liver cancer progression, we investigated the relationship between expression imbalance and tumor differentiation grade (Fig. 2).

First, we counted the expression-positive regions by expression imbalance map and arranged the samples according to the sum of positive regions. This resulted in the identification of 9 samples that constitute the first group and contain less than two positive regions, 10 samples in the second group with three or four positive regions, and 12 samples in the third group with more than five positive regions. Interestingly, all of the samples from the first group were well differentiated, and all of the poorly differentiated samples were concentrated in the third group (Fig. 2*A*), demonstrating a distinct trend for poorly differentiated grade tumors to contain more chromosomal aberrations.

Summating the number of 100-kb regions with expression imbalance, tumor differentiation grade and total length of chromosomal change were significantly correlated: the mean length of expression changes were 9.7 ± 5.6, 28.3 ± 13.0, and 45.2 ± 7.9 Mb in well differentiated, moderately differentiated, and poorly differentiated, respectively ($P < 0.00001$ by ANOVA; Fig. 2*B*). Some chromosomal regions showed consistent relationships with tumor progression. For example, expression gains of chromosome arms were observed on 12q23-24 and 20q11 with dedifferentiation from well differentiated to moderately differentiated, whereas an expression gain of 17q25 was significantly associated with dedifferentiation from well differentiated and moderately differentiated to poorly differentiated ($P < 0.05$ by Student-Newman-Keuls test). Notably, a gain of 17q12-21 and loss of 4q13 were found in each step of tumor dedifferentiation (Fig. 2*C*).

These results suggest that expression alterations of 1q21-23, 8p12-21, 8q13-21, and 17p13 occur as early events in hepatocarcinogenesis and 4q13, 12q23-24, 17q12-21, 17q25, and 20q11 as later events. Thus, liver cancer progresses with stepwise chromosomal expression change.

Expression Imbalance Map Was Correlated with Genomic Aberrations on 1q21-23 and 17p13 by Genomic qPCR. Many genomic aberrant regions in hepatocellular carcinoma detected by the expression imbalance map in this study are the same as those identified by CGH in previous studies (Table 2). To investigate the relationship between genomic and transcriptional aberrations, genome dosage in 1q21-23, 12q23-24, and 17p13 regions was confirmed using genomic qPCR for 27 hepatocellular carcinoma and the corresponding noncancerous liver samples (15).

qPCR was performed using 27 noncancerous liver samples. Average copy numbers for the loci of *CCT3* and *PSMB4* genes were 1.28 ± 0.37 and 0.90 ± 0.22, respectively. The genome dosage of hepatocellular carcinoma tended to increase in accordance with tumor differentiation grade (Fig. 3, *A* and *B*). In particular, consistent with the expression imbalance map data ($P < 0.001$, Mann-Whitney *U* test), genome dosage, shown as relative quantification, was significantly increased in moderately differentiated and poorly differentiated compared with well differentiated, both in *CCT3* and *PSMB4*. To clarify the relationship between genome dosage and the probability of expression imbalance in the 1q21-23 region, the relative quantification between samples with E values < 3 was compared with those samples with E values > 3. As shown in the top right section of Fig. 3, the relative quantification of *CCT3* and *PSMB4* increased significantly in the higher E value group ($P < 0.05$, Mann-Whitney *U* test; Fig. 3, *A* and *B*).

Genomic loss was also detectable in 17p13 region. Consistent with the expression imbalance map data, relative quantification was significantly decreased in samples with E values > 2, compared with those with E values < 2, both in *ASGR1* and *DKFZP566H073* (Fig. 3, *C* and *D*), whereas genomic amplification on 12q23-24 was not observed by qPCR (data not shown).

Through these results, we demonstrated that genes identified by expression imbalance map had altered genome dosage with statistical significance, and alterations of their mRNA expression levels may reflect a gain or loss of genomic copy number at the locus from 147.4 to 158.1 Mb on 1q21-23 and from 2.5 to 7.7 Mb on 17p13. On the other hand, genome dosage of chromosome 12q23-24, which has never detected in the previous CGH, has no change between hepatocellular carcinoma and chronic liver disease in DNA using qPCR.

Search for Candidate Genes Responsible for Hepatocarcinogenesis and Liver Cancer Progression. To identify candidate genes responsible for hepatocarcinogenesis and liver cancer progression, we further investigated the transcription of each of 55 genes in the 1q21-23 region (147.4–158.1Mb; Fig. 4). We found four related genes that were highly expressed in hepatocellular carcinoma compared with noncancerous tissues, *HAX1* (1q22), *SHC1* (1q21), *CKS1B* (1q21), and *CCT3* (1q23). Similarly, two growth-related genes were identified on the other nine regions selected by expression imbalance map: *AATF* (17q11-12) and *TK1* (17q23-25) had increased expression compared with noncancerous tissues.

DISCUSSION

Using CGH, many investigators have already reported various chromosomal regions of hepatocellular carcinoma that undergo cytogenetic change (16–28). Consistent with the previous data, the expression imbalance map identified an increase in gene expression on chromosomes 1q, 8q, 17q, and 20q and a decrease on 4q, 8p, 13q, and 17p. To validate the relationship between expression imbalance and

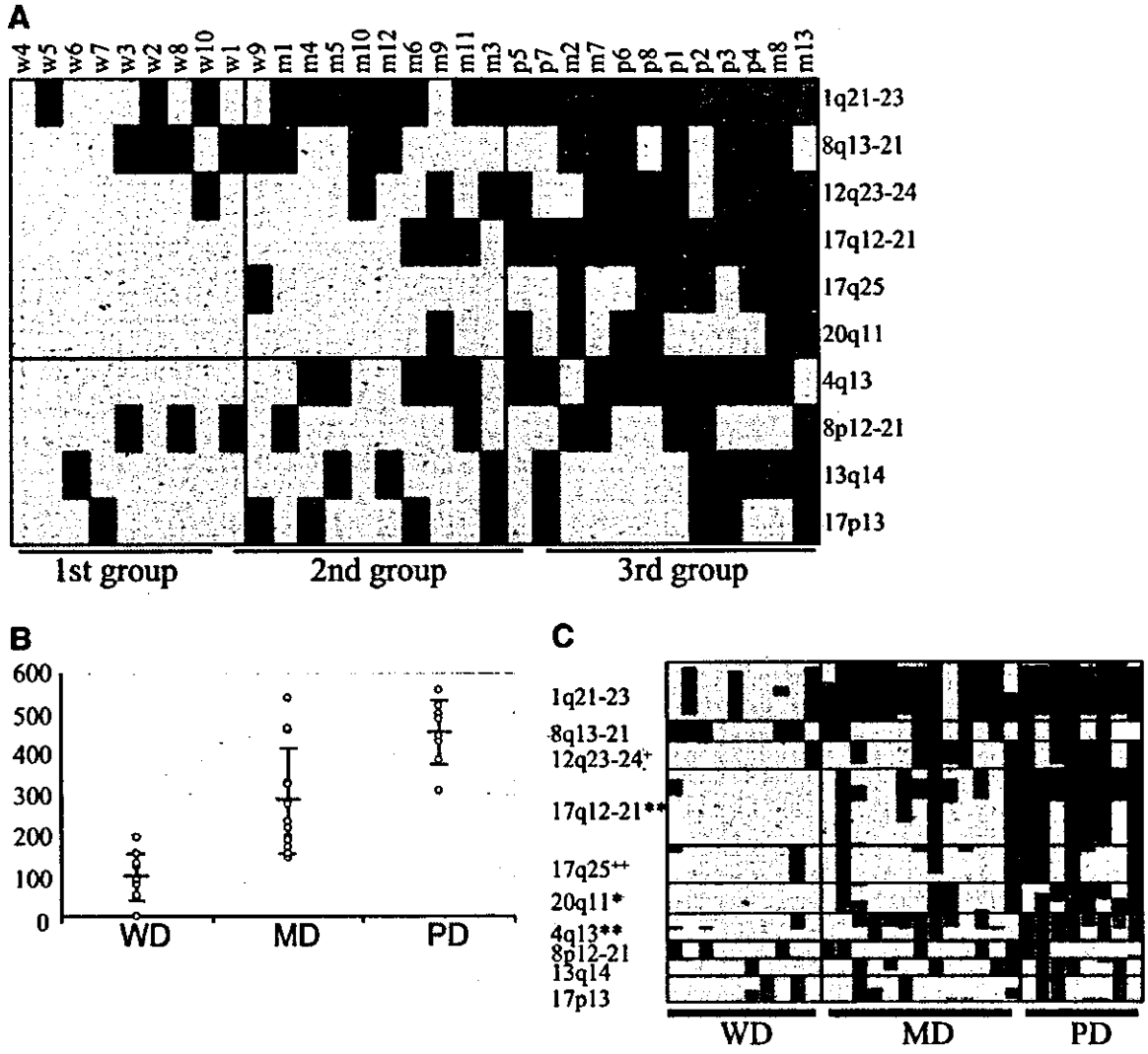

Fig. 2. Chromosomal bias of gene expression in liver cancer progression. *A*. Of 10 chromosomal regions selected by the expression imbalance map, the positive chromosomal regions were counted, and three groups were defined according to the sum of positive regions. Each column represents tissue samples and each row chromosomal regions. Relative expression levels in each chromosomal region are shown in *red* (high levels) and *blue* (low levels). *B*, chromosomal alteration in each tumor differentiation grade. Total amount of chromosomal alteration in 10 positive chromosomal regions by the expression imbalance map is increased as liver cancer develops. *Y* axis represents the total length of positive regions by the expression imbalance map (×100 kb). *C*, This analysis was carried out using 10 chromosomal regions selected by the expression imbalance map. Chromosomal change associated with each 100 kb is scored, and samples arranged according to the tumor differentiation grade. Each column represents tissue samples and each row chromosomal regions. Relative expression levels in each chromosomal region are shown in *red* (high) and *blue* (low). Statistical significance is considered as $P < 0.05$ by Mann-Whitney *U* test and shown on the left [*, statistical significance between well differentiated (WD) and moderately differentiated (MD); **, statistical significance in each differentiation grade of liver cancer; +, statistical significance between WD and MD + poorly differentiated (PD); ++, statistical significance between WD+MD and PD). Statistical significance is considered as $P < 0.05$.

genomic imbalance, we confirmed genomic aberration on chromosomes 1q21-23 and 17p13 using genomic qPCR. Specifically, all underexpressed regions 4q, 8p, 13q, and 17p have been identified by comprehensive allelotyping study (29–32), indicating that the regions with expression loss detected by expression imbalance map may be the result of loss of heterozygosity. In addition to the regions detected in previous CGH studies, we identified an expression gain in expression imbalance map at 12q23-24. The fact that 12q23-24 was identified only by the expression imbalance map and was not detected by both conventional methods and our data using qPCR suggests that there is no amplification of genome dosage but, rather, a transcriptional regulation because nine genes on 12q23-24 contain *MAZ*, *SP1*, and *E2F* binding sites in their upstream beyond expectation (data not shown). Thus, by using a new method without selective threshold processing in conjunction with a distribution-based algorithm, the expression imbalance map was able to detect regionally over- or underexpressed genes from gene expression data of oligonucleotide arrays with higher resolution than had been achieved previously (14). Furthermore, the expression imbalance map is based on microarray data and can, therefore, offer mRNA expression and expression imbalance information simultaneously.

Despite morphologic change, comprehensive expression profiling without expression imbalance map analysis fails to distinguish well differentiated from moderately differentiated.[6] In this study, using the expression imbalance map, we focused the gene alteration of differentiation grade of hepatocellular carcinoma. Expression gains of 1q21-23 and 8q13-21 and losses of 8p12-21 and 17p13 were observed in carcinogenesis from chronic liver disease to well differentiated, whereas up-regulation of 12q23-24, 17q12-21, 17q25, and 20q11 and a down-regulation of 4q13 were found only in moderately differentiated and poorly differentiated, although others reported that loss of 4q region occurred in various steps, *e.g.*, in the step from adenoma to well differentiated (33) or from well differentiated to moderately

[6] Unpublished observations.

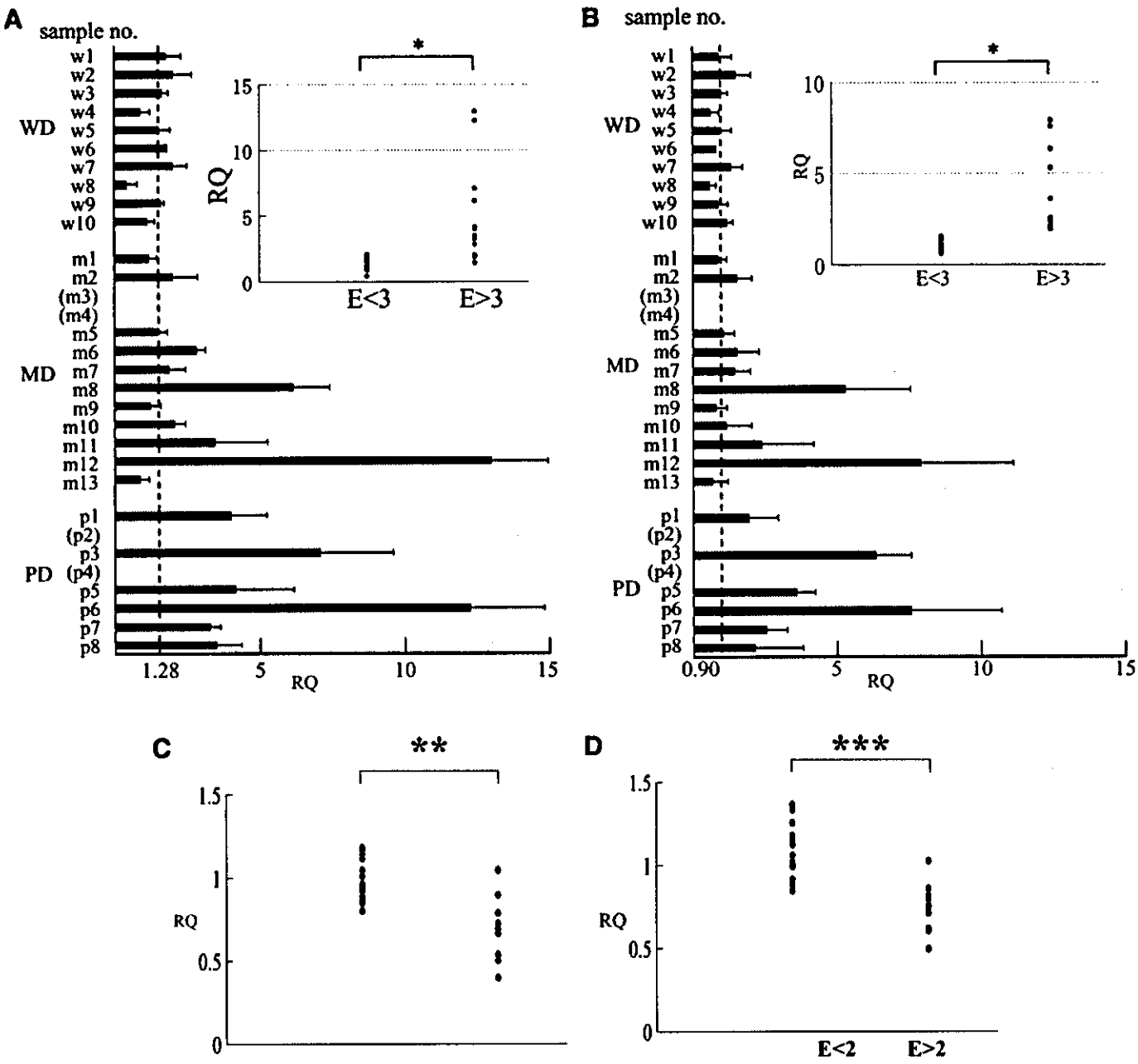

Fig. 3. Genomic imbalance of chromosome by qPCR. Genomic imbalance of chromosome 1q21-23 verified by qPCR applied to detecting copy number for liver cancer, according to differentiation grade. Amplification plots were obtained for *CCT3* and *PSMB4*, both of which were part of a highly expressed region identified by the expression imbalance map. Data are expressed as relative quantification (RQ) defined in Materials and Methods and are the mean ± SD of three determinations per experiment from three separate experiments. The *broken line* indicates the average of genome dosage of nondiseased area of livers (1.28 for *CCT3* and 0.90 for *PSMB4*). Genome dosage was compared between the two groups, an E value is <3, and >3 in the expression imbalance map, using the Mann-Whitney *U* test (shown in the top right side). (*, statistical significance was considered as $P < 0.05$). *A* in *CCT3* and *B* in *PSMB4*. Genome dosage was also compared between the two groups, an E value is <2 and >2 in expression imbalance map in 17p13 region. *C* in *ASGR1* and *D* in *DKFZP566H073*. (**, $P < 0.001$ and ***, $P < 0.0001$). Samples m3, m4, p2, and p4 were not determined because of lack of frozen specimens.

differentiated and poorly differentiated (34). These observations suggest that, including 17q12-21, which exhibits an imbalance of expression in each differentiation grade, chromosomal aberration of 4q, 12q, 17q12-21, 17q25, and 20q may play pivotal role in liver cancer progression. Our results further suggest that 1q, 8p, 8q, and 17p may be associated with initiation of hepatocarcinogenesis. Besides the chromosomal regions concerning in liver cancer progression described above, our data showed 13q14 region was concentrated on moderately differentiated and poorly differentiated, although there has no statistical significance ($P = 0.1652$), consistent with the previous reports by CGH or allelotype study (26, 34). In addition, Wilkens *et al.* (33) demonstrated that gains of 1q, 8q, and 16p and losses of 4q, 8p, and 17p were found in hepatocarcinogenesis, which were compatible to our data except for 4q and 16p. These results demonstrate a stepwise expression change in chromosomal loci correlating with hepatocellular carcinoma progression.

On 1q21-23, we focused on four growth-related genes: *HAX-1*, *SHC1*, *CKS1B*, and *CCT3*. *HAX-1* and *SHC1* have been demonstrated to induce activation of tyrosine kinases (35, 36), whereas *CKS1B* and *CCT3* may accelerate the cell cycle (37, 38). These expression gains of tyrosine kinase and cell cycle-related genes are consistent with the less differentiated, rapidly growing, liver cancer. Apart from 1q21-23, several genes that may be associated with liver cancer progression are clustered on 17q12-21 and 17q25. *AATF*, which interferes with the

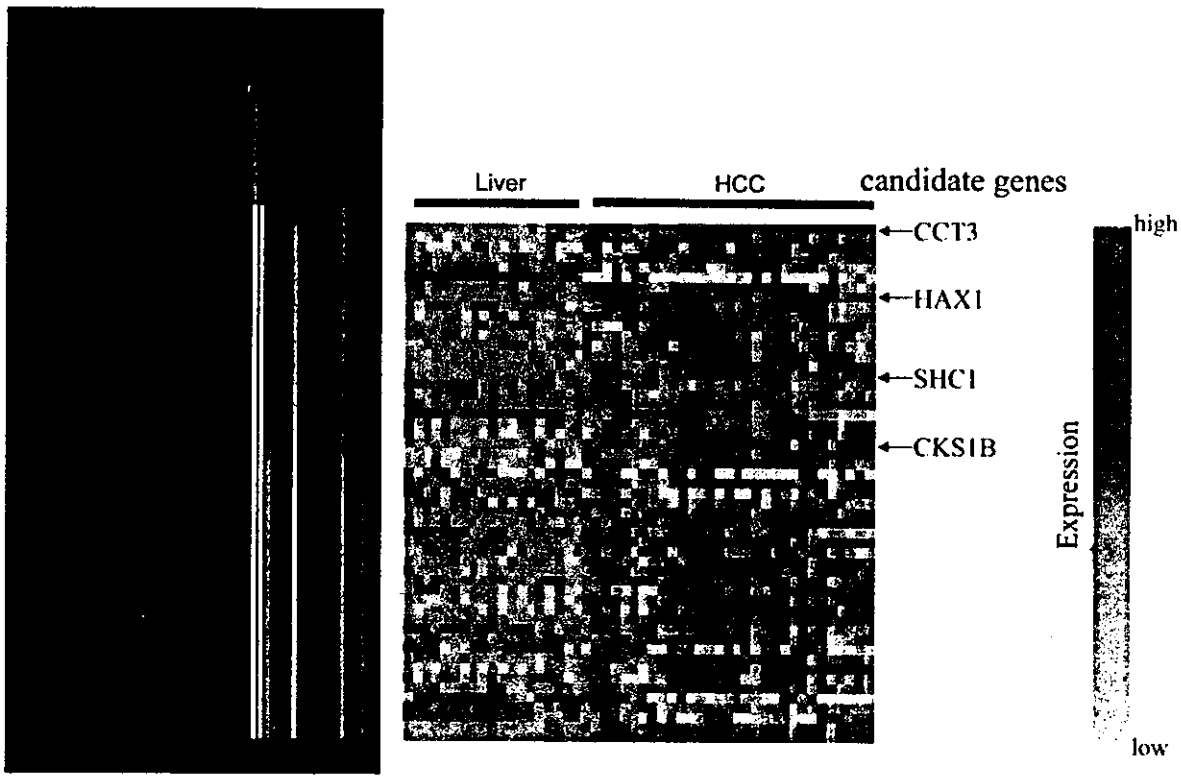

Fig. 4. Representative candidate genes responsible for liver cancer development in 1q21-23. The expression imbalance region at E value > 2 and range of an expression gain > 3.0 Mb in 1q21-23. The heat map shows relative expression levels of genes contained in the 1q21-23 region. Each column represents samples, and each row represents genes. The symbol of each candidate genes is shown on the right. Relative expression levels are shown in *red* (high) and *blue* (low).

induction of cell apoptosis through MAP3K/DLK (39), and *TK1*, a marker for the development for breast cancer (40), were also up-regulated in liver cancer.

We focused on expression change with chromosomal bias using the expression imbalance map, a recently developed method for the detection of mRNA expression imbalance regions. Comparison of expression imbalance map data with previous analysis of chromosomal imbalance identified by CGH and validation using qPCR indicate that gene expression profiles reflect chromosomal alteration. Furthermore, the expression imbalance map provides a direct measure of mRNA expression gain or loss that eliminates the need for confirmation of transcription levels of each gene. This method has the advantage that chromosomal bias and gene expression can be observed simultaneously with ease and reliability.

ACKNOWLEDGMENTS

We thank Hiroko Meguro and Aya Nonaka for valuable technical assistance, Shogo Yamamoto for excellent technical assistance and Yoshitaka Hippo for helpful discussion.

REFERENCES

1. Vogelstein B, Fearon ER, Hamilton SR, et al. Genetic alterations during colorectal-tumor development. N Engl J Med 1988;319:525–32.
2. Midorikawa Y, Tsutsumi S, Taniguchi H, et al. Identification of genes associated with dedifferentiation of hepatocellular carcinoma with expression profiling analysis. Jpn J Cancer Res 2002;93:636–43.
3. Chuma M, Sakamoto M, Yamazaki K, et al. Expression profiling in multistage hepatocarcinogenesis: identification of HSP70 as a molecular marker of early hepatocellular carcinoma. Hepatology 2003;37:198–207.
4. Kallioniemi A, Kallioniemi OP, Sudar D, et al. Comparative genomic hybridization for molecular cytogenetic analysis of solid tumors. Science (Wash. DC) 1992;258: 818–21.
5. Pollack JR, Perou CM, Alizadeh AA, et al. Genome-wide analysis of DNA copy-number changes using cDNA microarrays. Nat Genet 1999;23:41–6.
6. Pinkel D, Segraves R, Sudar D, et al. High resolution analysis of DNA copy number variation using comparative genomic hybridization to microarrays. Nat Genet 1998; 20:207–11.
7. Cai WW, Mao JH, Chow CW, Damani S, Balmain A, Bradley A. Genome-wide detection of chromosomal imbalances in tumors using BAC microarrays. Nat Biotechnol 2002;20:393–6.
8. DeRisi J, Penland L, Brown PO, et al. Use of a cDNA microarray to analyse gene expression patterns in human cancer. Nat Genet 1996;14:457–60.
9. Golub TR, Slonim DK, Tamayo P, et al. Molecular classification of cancer: class discovery and class prediction by gene expression monitoring. Science (Wash. DC) 1999;286:531–7.
10. Hippo Y, Taniguchi H, Tsutsumi S, et al. Global gene expression analysis of gastric cancer by oligonucleotide microarrays. Cancer Res 2002;62:233–40.
11. Tay ST, Leong SH, Yu K, et al. A combined comparative genomic hybridization and expression microarray analysis of gastric cancer reveals novel molecular subtypes. Cancer Res 2003;63:3309–16.
12. Mukasa A, Ueki K, Matsumoto S, et al. Distinction in gene expression profiles of oligodendrogliomas with and without allelic loss of 1p. Oncogene 2002;21:3961–8.
13. Virtaneva K, Wright FA, Tanner SM, et al. Expression profiling reveals fundamental biological differences in acute myeloid leukemia with isolated trisomy 8 and normal cytogenetics. Proc Natl Acad Sci USA 2001;98:1124–9.
14. Kano M, Nishimura K, Ishikawa S, et al. Expression imbalance map: a new visualization method for detection of mRNA expression imbalance regions. Physiol Genomics 2003;13:31–46.
15. Reis PP, Rogatto SR, Kowalski LP, et al. Quantitative real-time PCR identifies a critical region of deletion on 22q13 related to prognosis in oral cancer. Oncogene 2002;21:6480–7.
16. Chang J, Kim NG, Piao Z, et al. Assessment of chromosomal losses and gains in hepatocellular carcinoma. Cancer Lett 2002;182:193–202.
17. Kitay-Cohen Y, Amiel A, Ashur Y, et al. Analysis of chromosomal aberrations in large hepatocellular carcinomas by comparative genomic hybridization. Cancer Genet Cytogenet 2001;131:60–4.
18. Niketeghad F, Decker HJ, Caselmann WH, et al. Frequent genomic imbalances suggest commonly altered tumour genes in human hepatocarcinogenesis. Br J Cancer 2001;85:697–704.
19. Shiraishi K, Okita K, Kusano N, et al. A comparison of DNA copy number changes detected by comparative genomic hybridization in malignancies of the liver, biliary tract and pancreas. Oncology 2001;60:151–61.
20. Balsara BR, Pei J, De Rienzo A, et al. Human hepatocellular carcinoma is characterized by a highly consistent pattern of genomic imbalances, including frequent loss of 16q23.1-24.1. Genes Chromosomes Cancer 2001;30:245–53.

21. Tornillo L, Carafa V, Richter J, et al. Marked genetic similarities between hepatitis B virus-positive and hepatitis C virus-positive hepatocellular carcinomas. J Pathol 2000;192:307–12.
22. Wong N, Lai P, Pang E, et al. Genomic aberrations in human hepatocellular carcinomas of differing etiologies. Clin Cancer Res 2000;6:4000–9.
23. Guan XY, Fang Y, Sham JS, et al. Recurrent chromosome alterations in hepatocellular carcinoma detected by comparative genomic hybridization. Genes Chromosomes Cancer 2000;29:110–6.
24. Marchio A, Pineau P, Meddeb M, et al. Distinct chromosomal abnormality pattern in primary liver cancer of non-B, non-C patients. Oncogene 2000;19:3733–8.
25. Sakakura C, Hagiwara A, Taniguchi H, et al. Chromosomal aberrations in human hepatocellular carcinomas associated with hepatitis C virus infection detected by comparative genomic hybridization. Br J Cancer 1999;80:2034–9.
26. Kusano N, Shiraishi K, Kubo K, Oga A, Okita K, Sasaki K. Genetic aberrations detected by comparative genomic hybridization in hepatocellular carcinomas: their relationship to clinicopathological features. Hepatology 1999;29:1858–62.
27. Marchio A, Meddeb M, Pineau P, et al. Recurrent chromosomal abnormalities in hepatocellular carcinoma detected by comparative genomic hybridization. Genes Chromosomes Cancer 1997;18:59–65.
28. Wong N, Lai P, Lee SW, et al. Assessment of genetic changes in hepatocellular carcinoma by comparative genomic hybridization analysis: relationship to disease stage, tumor size, and cirrhosis. Am J Pathol. 1999;154:37–43.
29. Bluteau O, Beaudoin JC, Pasturaud P, et al. Specific association between alcohol intake, high grade of differentiation and 4q34–q35 deletions in hepatocellular carcinomas identified by high resolution allelotyping. Oncogene 2002;21:1225–32.
30. Nishimura T, Nishida N, Itoh T, et al. Comprehensive allelotyping of well-differentiated human hepatocellular carcinoma with semiquantitative determination of chromosomal gain or loss. Genes Chromosomes Cancer 2002;35:329–39.
31. Chan KL, Lee JM, Guan XY, Fan ST, Ng IO. High-density allelotyping of chromosome 8p in hepatocellular carcinoma and clinicopathologic correlation. Cancer (Phila.) 2002;94:3179–85.
32. Wong CM, Lee JM, Lau TC, Fan ST, Ng IO. Clinicopathological significance of loss of heterozygosity on chromosome 13q in hepatocellular carcinoma. Clin Cancer Res 2002;8:2266–72.
33. Wilkens L, Bredt M, Flemming P, Becker T, Klempnauer J, Kreipe HH. Differentiation of liver cell adenomas from well-differentiated hepatocellular carcinomas by comparative genomic hybridization. J Pathol 2001;193:476–82.
34. Okabe H, Ikai I, Matsuo K, et al. Comprehensive allelotype study of hepatocellular carcinoma: potential differences in pathways to hepatocellular carcinoma between hepatitis B virus-positive and -negative tumors. Hepatology 2000;31:1073–9.
35. Suzuki Y, Demoliere C, Kitamura D, Takeshita H, Deuschle U, Watanabe T. HAX-1, a novel intracellular protein, localized on mitochondria, directly associates with HS1, a substrate of Src family tyrosine kinases. J Immunol 1997;158:2736–44.
36. McGlade J, Cheng A, Pelicci G, Pelicci PG, Pawson T. Shc proteins are phosphorylated and regulated by the v-Src and v-Fps protein-tyrosine kinases. Proc Natl Acad Sci USA 1992;89:8869–73.
37. Ganoth D, Bornstein G, Ko TK, et al. The cell-cycle regulatory protein Cks1 is required for SCF(Skp2)-mediated ubiquitinylation of p27. Nat Cell Biol 2001;3: 321–4.
38. Won KA, Schumacher RJ, Farr GW, Horwich AL, Reed SI. Maturation of human cyclin E requires the function of eukaryotic chaperonin CCT. Mol Cell Biol 1998; 18:7584–9.
39. Page G, Lodige I, Kogel D, Scheidtmann KH. AATF, a novel transcription factor that interacts with Dlk/ZIP kinase and interferes with apoptosis. FEBS Lett 1999;462: 187–91.
40. O'Neill KL, Hoper M, Odling-Smee GW. Can thymidine kinase levels in breast tumors predict disease recurrence? J Natl Cancer Inst (Bethesda) 1992;84:1825–8.

[CANCER RESEARCH 64, 2418–2423, April 1, 2004]

Identification of Soluble NH_2-Terminal Fragment of Glypican-3 as a Serological Marker for Early-Stage Hepatocellular Carcinoma

Yoshitaka Hippo,[1] Kiyotaka Watanabe,[4] Akira Watanabe,[1] Yutaka Midorikawa,[5] Shogo Yamamoto,[2] Sigeo Ihara,[2] Susumu Tokita,[7] Hiroko Iwanari,[7] Yukio Ito,[7] Kiyotaka Nakano,[6] Jun-ichi Nezu,[6] Hiroyuki Tsunoda,[6] Takeshi Yoshino,[6] Iwao Ohizumi,[6] Masayuki Tsuchiya,[6] Shin Ohnishi,[4] Masatoshi Makuuchi,[5] Takao Hamakubo,[3] Tatsuhiko Kodama,[3] and Hiroyuki Aburatani[1]

[1]Genome Science Division, [2]Division of Dynamical Bioinformatics, and [3]Division of Molecular Biology and Medicine, Research Center for Advanced Science and Technology, The University of Tokyo, Tokyo, Japan; Departments of [4]Gastroenterology and [5]Hepato-Biliary-Pancreatic Surgery, Graduate School of Medicine, The University of Tokyo, Tokyo, Japan; [6]Chugai Pharmaceutical Co., Ltd., Shizuoka, Japan; and [7]Perseus Proteomics, Inc., Tokyo, Japan

ABSTRACT

For detection of hepatocellular carcinoma (HCC) in patients with liver cirrhosis, serum α-fetoprotein has been widely used, but its sensitivity has not been satisfactory, especially in small, well-differentiated HCC, and complementary serum marker has been clinically required. Glypican-3 (GPC3), a heparan sulfate proteoglycan anchored to the plasma membrane, is a good candidate marker of HCC because it is an oncofetal protein overexpressed in HCC at both the mRNA and protein levels. In this study, we demonstrated that its NH_2-terminal portion [soluble GPC3 (sGPC3)] is cleaved between Arg^{358} and Ser^{359} of GPC3 and that sGPC3 can be specifically detected in the sera of patients with HCC. Serum levels of sGPC3 were 4.84 ± 8.91 ng/ml in HCC, significantly higher than the levels seen in liver cirrhosis (1.09 ± 0.74 ng/ml; $P < 0.01$) and healthy controls (0.65 ± 0.32 ng/ml; $P < 0.001$). In well- or moderately-differentiated HCC, sGPC3 was superior to α-fetoprotein in sensitivity, and a combination measurement of both markers improved overall sensitivity from 50% to 72%. These results indicate that sGPC3 is a novel serological marker essential for the early detection of HCC.

INTRODUCTION

Hepatocellular carcinoma (HCC) is one of the most prevalent cancers worldwide, and its incidence is still increasing (1). Because HCC develops from cirrhotic liver after chronic infection with hepatitis virus B or C, patients with liver cirrhosis (LC) are advised to undergo periodical screening of serum α-fetoprotein (AFP) levels and liver ultrasound for the purpose of early detection of cancer (2). AFP is a glycoprotein expressed abundantly in fetal liver but not in normal adult liver and is re-expressed by HCC as it dedifferentiates from a premalignant lesion in the cirrhotic liver through well-differentiated (WD) and moderately differentiated (MD) HCC to poorly differentiated HCC (3). AFP has been used as a serum marker of HCC for more than 40 years. However, ultrasound imaging has been more effective lately in early detection of small WD HCC, in which AFP has yet to be elevated (4), highlighting the clinical need for novel sensitive serum markers for WD HCC.

Many previous studies have identified genes up-regulated in HCC compared with surrounding noncancerous lesions using differential display or cDNA subtraction (5–8). Recently, microarray studies on HCC presented gene lists containing a number of overexpressed genes (9–14). However, to determine whether a gene is a good candidate as a serological marker of WD HCC, it is crucial to determine the following: (*a*) whether it is overexpressed in WD HCC; (*b*) whether it is not expressed abundantly in other normal organs; and (*c*) whether it is detectable in the serum.

Overexpression of *GPC3* mRNA in HCC has been reported by ourselves and several other groups (15–18). Moreover, frequency of *GPC3* mRNA overexpression was significantly higher than that of elevated serum level and mRNA level of AFP in small HCC (16). We also observed frequent overexpression of *GPC3* in WD HCC compared with AFP with microarray analysis.[8] Together with minimal expression in normal organs (16, 19), GPC3 has, undoubtedly, previously existed as an attractive candidate marker of HCC. We showed previously using a monoclonal antibody (mAb) that GPC3 protein is also highly expressed in HCC (15). In this study, we further characterized GPC3 protein using a panel of newly generated mAbs and investigated whether it could be detected specifically in the sera of the patients with HCC. Finally, we successfully established a detection system for the soluble fragment of GPC3 (sGPC3) and confirmed its usefulness as a novel biomarker for HCC.

MATERIALS AND METHODS

Serum Samples. Serum samples were collected at Tokyo University Hospital with informed consent from 69 patients with HCC and 38 patients with LC, defined according to the following criteria: patients with a pathological diagnosis of HCC after surgery or with evidence of tumor stain on computed tomography or angiography were diagnosed with HCC; and patients diagnosed with LC were limited to those who had no history of HCC and no ultrasound evidence of tumor for more than 6 months from the day of serum collection.

Purification of Recombinant GPC3 Proteins. For protein expression, we used modified pCXN vector that contained dihydrofolate reductase expression unit as a selection marker. Original pCXN vector (20) was generously provided by J. Miyazaki (Osaka University Medical School, Osaka, Japan). An expression vector for GPC3 that lacks the COOH-terminal hydrophobic glycosylated phosphatidylinositol (GPI)-anchoring domain, GPC3ΔGPI, was constructed by introducing cDNA corresponding to amino acid residues 1–563 of GPC3 into modified pCXN with a FLAG tag added at the COOH terminus. An expression vector for GPC3ΔGPI without heparan sulfate, GPC3ΔGPIΔHS, was constructed by changing Ser^{495} and Ser^{509} to Ala to abolish the heparan sulfate attachment site. These constructs were stably transfected into Chinese hamster ovary cells deficient in the dihydrofolate reductase gene. Culture media containing GPC3ΔGPI-FLAG or GPC3ΔGPIΔHS-FLAG recombinant proteins were collected and loaded to DEAE ion-exchange chromatography DEAE Sepharose FF (Amersham Bioscience, Tokyo, Japan). After washing, eluted protein solutions were applied to anti-FLAG M2 antibody beads (Sigma, St.

Received 7/19/03; revised 11/25/03; accepted 1/12/04.

Grant support: Grants-in-Aid for Scientific Research (B) 12557051 and 13218019 and Scientific Research on Priority Areas (C) 12217031 from the Ministry of Education, Culture, Sports, Science and Technology; Health and Labor Sciences Research Grants for Research on Hepatitis and BSE from the Ministry of Health Labor and Welfare; and funds from Uehara Memorial Foundation (H. Aburatani). This study was carried out as a part of The Technology Development for Analysis of Protein Expression and Interaction in Bioconsortia on R&D of New Industrial Science and Technology Frontiers that was overseen by the Industrial Science, Technology and Environmental Policy Bureau, Ministry of Economy, Trade and Industry and delegated to New Energy Development Organization.

The costs of publication of this article were defrayed in part by the payment of page charges. This article must therefore be hereby marked *advertisement* in accordance with 18 U.S.C. Section 1734 solely to indicate this fact.

Requests for reprints: Hiroyuki Aburatani, Genome Science Division, Research Center for Advanced Science and Technology, The University of Tokyo, 4-6-1 Komaba, Meguro-ku, Tokyo 153-8904, Japan. Phone: 81-3-5452-5235; Fax: 81-3-5452-5355; E-mail: haburata-tky@umin.ac.jp.

[8] Y. Midorikawa, S. Tsutsumi, K. Nishimura, N. Kamimura, M. Kano, H, Sakamoto, M. Makuuchi, and H. Aburatani. Transcriptional Signature in Progression of Hepatocellular Carcinoma, manuscript in preparation.

Louis, MO). Proteins eluted with solution containing 200 μg/ml FLAG peptide (Sigma) were subjected to gel filtration chromatography with HiLoad 26/60 Superdex200pg (Amersham Bioscience). Finally, recombinant protein was concentrated using DEAE Sepharose FF.

Generation of Anti-GPC3 mAbs. We used recombinant GPC3ΔGPI as an immunogen. Spleen cells were isolated and fused with mouse myeloma P3-X63Ag8U1 cells (American Type Culture Collection, Manassas, VA). Hybridomas were selected by ELISA against the purified recombinant GPC3ΔGPIΔHS-FLAG, followed by cloning with limited dilution. Three mouse mAbs (A1836A, M18D04, and M19B11) were used in this study. For epitope mapping of these mAbs, a pGEX-5X (Amersham Biosciences) construct for the NH_2-terminal portion of GPC3 (amino acids 25–358) was expressed in *Escherichia coli* BL21 Codon Plus (DE3) pLys (Stratagene, La Jolla, CA) as a glutathione *S*-transferase-fusion protein and subject to immunoblotting analysis.

Immunoblotting. Total cell lysates were obtained after lysis in 10 mM Tris (pH 7.4), 150 mM NaCl, 5 mM EDTA, 1.0% Triton X-100, 1.0% sodium deoxycholate, and 0.1% SDS with protease inhibitor mixture (Sigma). Culture supernatant was obtained from serum-free medium used for culture of hepatoma cells. Proteins were separated with 12% SDS-PAGE and transferred to polyvinylidene difluoride Hybond P membrane (Amersham Biosciences). The membrane was treated with 2% nonfat milk in TBS containing 0.05% Tween 20 (TBST) followed by incubation with anti-GPC3 mAb in TBST and subsequent incubation with horseradish peroxidase-conjugated secondary antibody (dilution, 1:5000; Amersham Biosciences) in TBST. The protein was visualized using the enhanced chemiluminescence plus detection system (Amersham Biosciences).

Immunoprecipitation. We first prepared antibody beads by covalently linking 25 μl of protein G-Sepharose (Amersham Biosciences) and 50 μg of anti-GPC3 mAb M18D04 or M19B11 with 20 mM dimethyl pimelimidate (ICN Aurora, Aurora, OH). We then added 50 μl of sera from the patients or culture media of HuH7 cells diluted in 250 μl with PBS to 25 μl of antibody beads and incubated them for 2 h at 4°C. After extensive washing with PBS, antibody beads were boiled for 5 min in 50 μl of SDS-PAGE loading buffer containing 10% 2-mercaptoethanol, and subsequently, immunoblotting was performed.

Sandwich ELISA. One μg of anti-GPC3 mAb A1836A per well was immobilized to 96-well plate Maxisorp (Nalge Nunc International, Roskilde, Denmark) and stabilized with Immunoassay Stabilizer (Advanced Biotechnologies Inc., Columbia, MD). Twenty-five μl of sera or standard were diluted with 100 μl of buffer containing 20% normal rabbit serum (Pel-Freez Biologicals, Rogers, AR), 1% BSA (Oriental Yeast Co., Ltd., Osaka, Japan), and 2% mouse ascites Hyb-3423 (Institute of Immunology, Tokyo, Japan) in 50 mM Tris-Cl (pH 8.0), 0.15 M NaCl, and 1 mM EDTA and incubated at room temperature for 2 h. After washing, 25 μl of biotinylated antibody solution containing anti-GPC3 mAbs M18D04 (1.88 μg/ml) and M19B11 (3.75 μg/ml) and 100 μl of horseradish peroxidase-labeled streptavidin (Vector Laboratories Inc., Burlingame, CA) were added to the plate and incubated twice at room temperature for 30 min. TMB Soluble Reagent and Stop Buffer (Scy Tek Laboratories, Inc., Logan, UT) were added as substrate, and absorbance at 450 nm was read with EIA Reader (Corona Electric Co., Ltd., Ibaraki, Japan). Recombinant GPC3ΔGPI was used as a standard sample in each assay.

Amino Acid Sequence Analysis. Recombinant GPC3ΔGPI and GPC3ΔGPIΔHS were purified and separated by SDS-PAGE and transferred to polyvinylidene difluoride membrane ProBlott (Applied Biosystems, Foster City, CA). The membrane was stained with CBB R-250, and sections containing bands of M_r 40,000 and M_r 30,000 were cut out separately. These polyvinylidene difluoride membrane sections were washed with a solution including 50% acetonitrile and 0.1% trifluoroacetic acid and applied to an ABI 492 Protein Sequencer (Applied Biosystems) to sequence the NH_2 terminus of the protein. Because the NH_2 terminus of the M_r 40,000 protein was blocked, the membrane was further incubated in acetate with 0.6 mg/ml 3-bromo-3-methyl-2-nitrophenyl-mecapto-3*H*-indole (ICN Biomedicals Inc., Irvine, CA) at 80°C for 1 h in the dark to chemically cleave the protein at the COOH terminus of tryptophan residues. After washing twice with 80% acetate and once with 10% methanol, the peptide was analyzed using an ABI 492 Protein Sequencer. The detected sequence was aligned using FASTS software available online,[9] and the protein was identified.

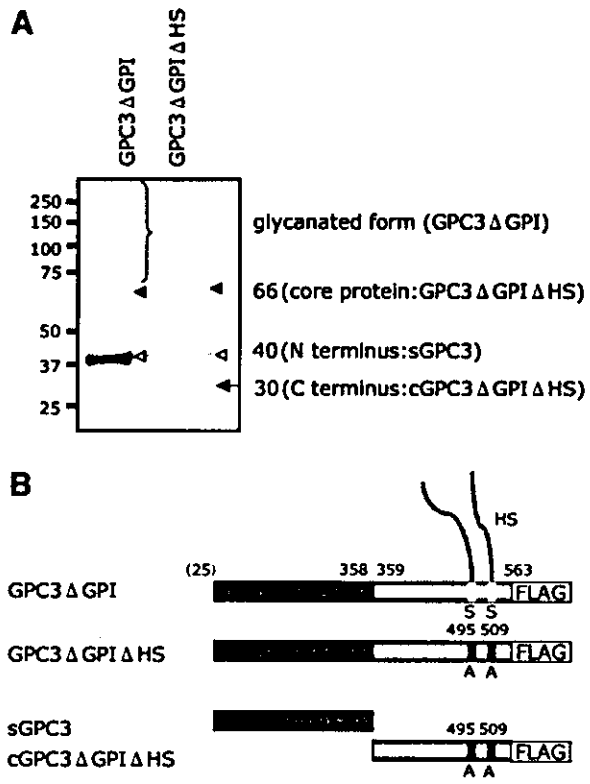

Fig. 1. Characterization of recombinant glypican-3 (GPC3) proteins. *A*, CBB R-250-stained SDS-PAGE of purified recombinant GPC3. *Brace*, glycanated GPC3 (smearing), GPC3ΔGPI; *closed arrowhead*, core protein of GPC3 (M_r 66,000) that lacks heparan sulfate glycosaminoglycan, GPC3ΔGPIΔHS; *open arrowhead*, sGPC3 (M_r 40,000); *arrow*, cGPC3ΔGPIΔHS (M_r 30,000). *B*, schematic diagram of recombinant proteins. *Numbers above the boxes* indicate amino acid residue number. Note that NH_2-terminal residue 25 is putative and indicated in *parentheses*. *HS*, heparan sulfate glycosaminoglican.

RESULTS

The NH_2-Terminal Portion of GPC3 Is Cleaved between Arg^{358} and Ser^{359} *in Vitro*. We have previously generated mAb K6534 raised against a peptide corresponding to amino acids 355–371 of GPC3 protein, and we demonstrated, for the first time, overexpression of its core protein in HCC with immunoblotting using this antibody (15). Another antibody is required to construct a sandwich ELISA system for serum examination of GPC3, so we started generating high-affinity mAbs using recombinant GPC3ΔGPI as an immunogen. While purifying the immunogen from the culture supernatant of Chinese hamster ovary cells, we observed a M_r 40,000 band (Fig. 1*A*) in addition to the M_r 66,000 band that corresponds to core protein of GPC3 as observed with K6534 (15).

Because the NH_2 terminus of this M_r 40,000 band was modified, as revealed by initial amino acid sequencing, we performed sequencing of internal amino acids of the band after cleavage at the COOH terminus of tryptophan residues to verify its origin. We detected six cycles of three amino acid residues VRY, EPX, YES, ITY, LPX, and QSV, each cycle corresponding to the first to sixth residue following tryptophan (W), respectively. After alignment with FASTF algorithm, these sequences matched with the (W)VPETPV (amino acid 51–57), (W)YCSYCQ (amino acid 261–267), and (W)REYILS (amino acid

[9] http://fasta.bioch.virginia.edu/.